THE JOURNAL OF BIOLOGICAL CHEMISTRY
Vol. 276, No. 41, Issue of October 12, pp. 38010–38022, 2001

Printed in U.S.A.

Novel Transcriptional Regulation of the Human *CYP3A7* Gene by Sp1 and Sp3 through Nuclear Factor κB-like Element*

Received for publication, July 2, 2001
Published, JBC Papers in Press, August 8, 2001, DOI 10.1074/jbc.M106130200

Tetsuya Saito, Yoshiki Takahashi, Hisashi Hashimoto, and Tetsuya Kamataki‡

From the Laboratory of Drug Metabolism, Graduate School of Pharmaceutical Sciences, Hokkaido University, N12W6, Kita-ku, Sapporo, Hokkaido 060-0812, Japan

Human CYP3A7 and CYP3A4 are expressed in fetal and adult livers, respectively, although the 5′-flanking regions of the two genes show 90% homology. The purpose of this study was to clarify the mechanism(s) responsible for the transcriptional regulation of the *CYP3A7* gene in human hepatoma HepG2 cells that showed fetal phenotypes. Transfection studies using a series of the *CYP3A7* or *CYP3A4* promoter-luciferase chimeric genes identified a nuclear factor κB (NF-κB)-like element between nucleotides −2326 and −2297 that conferred the transcriptional activation of the *CYP3A7* gene. A 1-base pair mismatch within the corresponding region of the *CYP3A4* gene was sufficient for a differential enhancer activity. A gel shift assay using nuclear extracts from HepG2 cells showed that Sp1 and Sp3 bound to the NF-κB-like element of the *CYP3A7* but not *CYP3A4* gene. Specific activation of the *CYP3A7* promoter by Sp1 and Sp3 was confirmed by a co-transfection of the p3A7NF-κB or p3A4NF-κB reporter gene with Sp1 or Sp3 expression plasmid into *Drosophila* cells, which lacked endogenous Sp family. Additionally, introduction of mutations into binding sites for hepatocyte nuclear factor 3β, upstream stimulatory factor 1, and a basic transcription element in the proximal promoter attenuated luciferase activity to 20% of the level seen with the intact *CYP3A7* promoter. Thus, we conclude that the expression of the *CYP3A7* gene in HepG2 cells is cooperatively regulated by Sp1, Sp3, hepatocyte nuclear factor 3β, and upstream stimulatory factor 1.

Cytochrome P-450 (CYP)[1] is responsible for the metabolism of a wide variety of xenobiotics and endogenous substrates (1). Multiple forms of CYP have been shown to be present in the liver (2). Among the forms of CYPs, CYP3A is the most abundant form in human livers (3, 4). The human CYP3A subfamily consists of four members: CYP3A4 (5–7), CYP3A5 (8, 9), CYP3A7 (10), and CYP3A43 (11).

Human CYP3A7 catalyzes the 16α-hydroxylation of dehydroepiandrosterone 3-sulfate and the 6β-hydroxylation of testosterone (12, 13). This enzyme was first purified and cloned by us from human fetal livers (10, 14). Our studies using Chinese hamster lung fibroblast cells stably transfected with a CYP3A7 expression plasmid and using transgenic mice that carried a CYP3A7 cDNA indicated that the enzyme was also responsible for the bioactivation of some carcinogens such as aflatoxin B_1 and sterigmatocystin (15–17).

The nucleotide sequence of the CYP3A7 (10) cDNA shares 94.2, 88.5, and 82.2% identities with those of CYP3A4 (5–7), CYP3A5 (8, 9), and CYP3A43 (11) cDNAs, respectively. Northern blot analysis using CYP3A7 or CYP3A4 cDNA as a probe and total RNAs prepared from human fetal and adult livers demonstrated that CYP3A7 and CYP3A4 mRNAs were expressed specifically in human fetal and adult livers, respectively (18). It has also been reported that a trace amount of CYP3A7 mRNA could be detected in some adult livers (19). CYP3A7 mRNA was detectable at 50–60 days of gestation (20). This expression reached a maximal level within a week after birth and then declined (21). Reciprocally, the expression of CYP3A4 mRNA was not seen in human fetal livers and began to increase after birth (21). The molecular mechanism(s) underlying the age-related expression of the *CYP3A7* and *CYP3A4* genes, however, has not yet been elucidated.

As reported previously, we isolated genomic clones containing the 5′-flanking region and the 13 exons spanning ~30 kb of the *CYP3A7* or *CYP3A4* gene (22, 23). The structures of exon-intron junctions of the *CYP3A7* and *CYP3A4* genes were highly conserved between the two genes. In addition, a 5′-flanking region from −1 kb to the transcriptional start site of the *CYP3A7* gene was 91% identical to that of the *CYP3A4* gene. In the same series of studies, we found characteristic sequences termed "HFLaSE" (P-450 HFLa-specific element) and "NFSE" ($P\text{-}450_{NF}$-specific element) in the 5′-flanking region of the *CYP3A7* and *CYP3A4* genes, respectively. However, we could not detect any age-related factors in gel shift assays using these elements as probes and nuclear extracts prepared from human fetal and adult livers. Thus, it appeared that a possible *cis*-acting element(s) responsible for the developmental transcription of the *CYP3A7* or *CYP3A4* gene was located in regions with minor differences or far upstream regions of the two genes.

The expression of the *CYP3A* genes is inducible by a wide variety of clinically important drugs, including rifampicin, dexamethasone, and clotrimazole (24). Recently, a human orphan nuclear receptor termed PXR, steroid and xenobiotic receptor, or pregnane-activated receptor that mediates the induction of CYP3As has been found (25–27). The PXR/retinoid X receptor

* This work was supported in part by grants-in-aid from the Ministry of Education, Science, Sports and Culture of Japan, from the Program for Promotion of Fundamental Studies in Health Sciences of the Organization for Drug ADR Relief, R&D Promotion, and from Product Review of Japan and the Core Research for Evolutional Science and Technology. The costs of publication of this article were defrayed in part by the payment of page charges. This article must therefore be hereby marked "*advertisement*" in accordance with 18 U.S.C. Section 1734 solely to indicate this fact.

‡ To whom all correspondence should be addressed: Lab. of Drug Metabolism, Graduate School of Pharmaceutical Sciences, Hokkaido University, N12W6, Kita-ku, Sapporo, Hokkaido 060-0812, Japan. Tel. and Fax: 81-11-706-4978; E-mail: kamataki@pharm.hokudai.ac.jp.

[1] The abbreviations used are: CYP, cytochrome P-450; BTE, basic transcription element; C/EBP, CCAAT/enhancer-binding protein; COUP-TF, chicken ovalbumin upstream promoter-transcription factor; HNF, hepatocyte nuclear factor; Igκ, immunoglobulin κ light chain; kb, kilobase(s); NF1, nuclear factor 1; NF-κB, nuclear factor κB; PCR, polymerase chain reaction; PXR, pregnane X receptor; RT, reverse transcriptase; SL2, Schneider line 2; USF, upstream stimulatory factor; YY1, ying yang 1.

heterodimer has been reported to interact with a PXR-responsive element that contains the everted repeat of an imperfect AGGTCA motif separated by 6 nucleotides (called as ER6). This element was identified in the proximal promoters of the *CYP3A4* and *CYP3A7* genes (25–28). Because the loss of the expression of PXR protein does not alter the constitutive expression of murine CYP3A proteins (29), a transcription factor(s) other than PXR is assumed to contribute to the constitutive expression of the *CYP3A* genes in mammals.

In an attempt to analyze the function of a promoter expressed in human fetal livers, human hepatoblastoma HepG2 cells have been used, because the cells show fetal hepatic phenotypes such as the increased synthesis of α-fetoprotein, fetal aldolase, and pyruvate kinase and the reduced synthesis of albumin (30). Successful results obtained so far suggest that HepG2 cells possess transcription factors necessary for the gene expression seen in the fetus. Thus, in the present study, HepG2 cells were employed and transiently transfected with a reporter plasmid in which the 5′-flanking region of the *CYP3A7* or the *CYP3A4* gene was fused to the luciferase gene to identify a possible *cis*-acting element(s) specifically responsible for the expression of the *CYP3A7* gene.

In this paper, we provide lines of evidence showing that the expression of CYP3A7 in HepG2 cells is coordinately regulated by HNF-3β, USF1, and the Sp (specificity protein) family members, which bind to the NF-κB-like element of the *CYP3A7* gene.

EXPERIMENTAL PROCEDURES

Cell Culture—Human hepatoma cells, HepG2 and HuH-7, were purchased from Riken (Tsukuba, Japan). *Drosophila* SL2 cells were purchased from Invitrogen (Groningen, The Netherlands). HepG2 and HuH-7 cells were maintained in Dulbecco's modified Eagle's medium (Nissui Pharmacy, Tokyo, Japan) supplemented with 10% fetal bovine serum (BioWhittaker, Walkersville, MD), nonessential amino acids (ICN, Aurora, OH), and 1 mM sodium pyruvate (Life Technologies, Inc.) at 37 °C in 5% CO_2. *Drosophila* SL2 cells were maintained in Schneider's medium (Life Technologies, Inc.) supplemented with 10% fetal bovine serum at 26 °C in 5% CO_2.

RNA Preparation and RT-PCR—Total RNAs were prepared from human hepatoma cells according to an acid guanidinium thiocyanate/phenol/chloroform method (31). To examine the expression levels of CYP3A7 and CYP3A4 mRNAs in HepG2 and HuH-7 cells, RT-PCR was performed as described previously (32). Briefly, total RNA (1 μg) and oligodeoxythymidylic acid primer (0.5 μg) were mixed. The RNA-primer mixture was incubated at 70 °C for 10 min and then cooled on ice. Subsequently, Moloney murine leukemia virus RT (20 units) (Toyobo, Tokyo, Japan), RNase inhibitor (20 units) (Takara, Tokyo, Japan), and 0.5 mM each of four deoxynucleoside triphosphates were added to the RNA-primer mixture and then incubated at 42 °C for 50 min. PCR was performed in a solution containing cDNA synthesized in a solution containing the above RT reaction mixture (1 μl), 1.5 mM $MgCl_2$, 0.2 mM each of four deoxynucleoside triphosphates, each primer (50 pmol), AmpliTaq Gold polymerase (2.5 units) (PerkinElmer Life Sciences), and 10× AmpliTaq reaction buffer (5 μl) (PerkinElmer Life Sciences). The reaction was performed for 30 cycles at 94 °C for 1 min, at 55 °C for 1 min, and at 72 °C for 2 min. The PCR products were subjected to a 2% agarose gel and then visualized by ethidium bromide staining. The sequences of primers used for RT-PCR are as follows: CYP3A7, 5′-CTATGATACTGTGCTACAGT-3′ and 5′-TCAGGCTCCACTTACGGTCT-3′; CYP3A4, 5′-CCAAGCTATGCTCTTCACCG-3′ and 5′-TCAGGCTCCACTTACGGT GC-3′; and glyceraldehyde-3-phosphate dehydrogenase, 5′-ACCACAGTCCATGCCATCAC-3′ and 5′-TCCACCAC CCTGTTGCTGTA-3′.

Construction of Plasmids—The oligonucleotide primers used for the synthesis of DNA fragments or for a site-directed mutagenesis are as follows: 3A7-S, 5′-TTCACTTGGCCACTGGAAGT-3′; 3A7-*Hin*dIII, 5′-TGAGAAGCTTCACTACTTTCCTTCCT-3′; 3A4-S, 5′-TGGACAGCCTGTCCACTGAT-3′; 3A4-*Hin*dIII, 5′-TGAGAAGCTTCACTACTTTCCTTACT-3′; 3A7/4–5.0 *Xho*I, 5′-CCTCGAGGT CTATAAAGTAT-3′; 3A7/4–4.5 *Xho*I, 5′-CCTCGAGGCTCTGGCCACTA-3′; 3A7/4–4.0 *Xho*I, 5′-CCTCGAGGGAGCTGTTGGTC-3′; 3A7/4–3.5, 5′-CCTCGAGGTGCCC TGAACAC-3′; 3A7/4–3.0, 5′-CCTCGAGGTAGATACCACGT-3′; 3A7/4-AS, 5′-ACCTCTCTTCTGGGAAGCTT-3′; 3A7–2.5 *Xho*I, 5′-CCTCGAGGCCATGTGCTTAGGGT ACAAA-3′; 3A7–2.47 *Xho*I, 5′-CCTCGAGGAGACCAAGAATAATGTCTGGGAG CACAATA-3′; 3A7–2.41 *Xho*I, 5′-CCTCGAGGTAATACAGGAAATGAG-3′; 3A7–2.35 *Xho*I, 5′-CCTCGAGGATCTTCCTTGACACAG-3′, 3A7–2.30 *Xho*I, 5′-CCTCGAGGC ATGTTAGAAGATGTTAC-3′; 3A7–2.0 *Xho*I, 5′-CCTCGAGGAAAGGCTCTTTGTTTAGGTG-3′; 3A7–1.5 *Xho*I, 5′-CCTCGAGGATGTACCAGAATTCCCTGGA-3′; 3A7–1.0 *Xho*I, 5′-CCTCGAGGCATGCAGTATTTCCAGAGAG-3′; 3A7–140 *Xho*I, 5′-CCTCGAGGTGTGTGATTATTTGCCAACT-3′; 3A7–90 *Xho*I, 5′-CCTCGAGG CTGCAGGCAGAGCACGGGGGCCCTGCTAC-3′; 3A7–35 *Xho*I, 5′-CCTCGAG GCTCCAGCATATA-3′; 3A4–2.5 *Xho*I, 5′-CCTCGAGGCTATGTGCTTAGGGTACAAA-3′; 3A4–2.0 *Xho*I, 5′-CCTCGAGGAAAGGCTCTCGGTTTAGGTG-3′; 3A4–1.5 *Xho*I, 5′-CCTCGAGGATGTATCAGAATTCCCTGGA-3′; 3A4–1.0 *Xho*I, 5′-CCTCGAGGCATGCAGTATTTCCAGAGAG-3′; 3A4–140 *Xho*I, 5′-CCTCGAGGTG TGTGATTCTTTGCCAACT-3′; 3A4–90 *Xho*I, 5′-CCTCGAGGCTGCAGGCAGA GCACAGGTGGCCCTGCTAC-3′; 3A7/4–2.25 *Xho*I, 5′-CCTCGAGGTCTGCCA CTTAATTCCAC-3′; 3A7NF-κB-S, 5′-CAGCTCTCAGTAGGCAAGTCCCTACA TGTT-3′; 3A7NF-κB-AS, 5′-AACATGTAGGGACTTGCCTACTGAGAGCTG-3′; 3A4NF-κB-S, 5′-CAGCTCTCAGTAGTCAAGTCCCTACATGTT3′; 3A4NF-κB-AS, 5′-AACATGTAGGGACTTGACTACTGAGAGCTG-3′; 3A4–140/−120-S, 5′-TGTGTG ATTCTTTGCCAACT-3′; 3A4–140/−120-AS, 5′-AGTTGGCAAAGAATCACACA-3′; 3A7NF1mut-.-S, 5′-TGTGTCATTATTTGCGAACT-3′; 3A7NF1mut.-AS, 5′-AGTTCGCA AATAATGACACA-3′; 3A4E-box-S, 5′-CTGCAGGCAGAGCACAGGTGGCCCT GCTAC-3′; 3A4E-box-AS, 5′-GTAGCAGGGCCACCTGTGCTCTGCCTGCAG-3′; 3A7USFmut.-S, 5′-CTGCAGGCAGAGCATAAGGGCCCTGCTAC-3′; 3A7USFmut.-AS, 5′-GTAGCAGGGCCCTTATGCTCTGCCTGCAG-3′; 3A7/4BTEmut.-S, 5′-CTCCAGCG AGGCCTCCTTCT-3′; and 3A7/4BTEmut.-AS, 5′-AGAAGGAGGCCTCGCTGGAG-3′.

Reporter plasmid p3A7/−5.5, which contained the 5′-flanking region from nucleotides −5564 to +105 (abbreviated to −5564/+105) relative to the transcriptional start site (22) of the *CYP3A7* gene, was constructed by ligation of the following three DNA fragments: (i) an *Xho*I/*Hin*dIII fragment (−5564/−2800) from the λHFLa11–44 (22); (ii) a *Hin*dIII fragment (−2800/+105) obtained by means of PCR using oligonucleotide primers, 3A7-S and 3A7-*Hin*dIII, and the λHFLa11–44 (22) as a template; and (iii) an *Xho*I/*Hin*dIII fragment from a control luciferase reporter plasmid, Basic Vector 2 (Toyoinki, Tokyo, Japan). Reporter plasmid p3A4/−5.5, which contained the 5′-flanking region (-5551/+105) of the *CYP3A4* gene (23), was constructed by ligation of the following three DNA fragments: (i) an *Xho*I/*Eco*RV fragment (−5551/−2700) from the λNF-32 (23); (ii) a *Eco*RV/*Hin*dIII fragment (−2700/+103) obtained by PCR using oligonucleotide primers, 3A4-S and 3A4-*Hin*dIII, and the λNF-32 (23) as a template; and (iii) an *Xho*I/*Hin*dIII fragment from Basic Vector 2. To construct reporter plasmids p3A7/−5.0, p3A7/−4.5, p3A7/−4.0, p3A7/−3.5, and p3A7/−3.0, PCR was performed using 3A7/4–5.0 *Xho*I, 3A7/4–4.5 *Xho*I, 3A7/4–4.0 *Xho*I, 3A7/4–3.5 *Xho*I, or 3A7/4–3.0 *Xho*I as a sense primer and 3A7/4-AS as an antisense primer. Synthesized fragments were digested with restriction enzymes *Xho*I and *Hin*dIII. Resultant fragments were inserted into the *Xho*I/*Hin*dIII site of p3A7/−5.5. To generate reporter plasmids p3A4/−5.0, p3A4/−4.5, p3A4/−4.0, p3A4/−3.5, and p3A4/−3.0, PCR was carried out using 3A7/4–5.0 *Xho*I, 3A7/4–4.5 *Xho*I, 3A7/4–4.0 *Xho*I, 3A7/4–3.5 *Xho*I, or 3A7/4–3.0 *Xho*I as a sense primer and 3A7/4-AS as an antisense primer. Synthesized fragments were cleaved with *Xho*I and *Hin*dIII. Resultant fragments were inserted into the *Xho*I/*Hin*dIII site of p3A4/−5.5. To generate reporter plasmids p3A7/−2.5, p3A7/−2.47, p3A7/−2.41, p3A7/−2.35, p3A7/−2.30, p3A7/−2.0, p3A7/−1.5, p3A7/−1.0, p3A7/−140, p3A7/−90, p3A7/−35, p3A4/−2.5, p3A4/−2.0, p3A4/−1.5, p3A4/−1.0, p3A4/−140, and p3A4/−90, PCR was performed using 3A7–2.5 *Xho*I, 3A7–2.47 *Xho*I, 3A7–2.41 *Xho*I, 3A7–2.35 *Xho*I, 3A7–2.30 *Xho*I, 3A7–2.0 *Xho*I, 3A7–1.5 *Xho*I, 3A7–1.0 *Xho*I, 3A7–140 *Xho*I, 3A7–90 *Xho*I, 3A7–35 *Xho*I, 3A4–2.5 *Xho*I, 3A4–2.0 *Xho*I, 3A4–1.5 *Xho*I, 3A4–1.0 *Xho*I, 3A4–140 *Xho*I, or 3A4–90 *Xho*I as a sense primer and 3A7-*Hin*dIII or 3A4-*Hin*dIII as an antisense primer. Synthesized fragments were digested with *Xho*I and *Hin*dIII. Resultant fragments were inserted into the *Xho*I/*Hin*dIII site of Basic Vector 2. Reporter plasmids p3A7/−580, p3A4/−580, p3A7/−360, p3A4/−360, p3A7/−62, and p3A4/−62 were generated by the cleavage of p3A7/−1.0 or p3A4/−1.0 with restriction enzymes *Sac*I, *Bgl*II, and *Pst*I, respectively. To construct reporter plasmids p3A7Ewild and p3A4Ewild, a region from −2.50 to −2.25 kb was amplified by PCR using 3A7–2.5 *Xho*I or 3A4–2.5 *Xho*I as a sense primer and 3A7/4–2.25 *Xho*I as an antisense primer. Synthesized fragments were digested with *Xho*I and then inserted into the *Xho*I site of p3A7/−62. The direction of

the inserts was confirmed by a sequence analysis (ABI PRISM™ 377; PerkinElmer Life Sciences). Reporter plasmids p3A7Emut. and p3A4Emut. were produced by site-directed mutagenesis using 3A4NF-κB-S, 3A4NF-κB-AS, 3A7NF-κB-S, and 3A7NF-κB-AS as mutated primers. To construct p3A7NF-κB or p3A4NF-κB, double-stranded 3A7NF-κB or 3A4NF-κB was introduced into the *Sma*I site of p3A7/−62. The copy number of the introduced oligonucleotides was confirmed by a sequence analysis. Reporter plasmids p3A7/−140/HNF-3mut., p3A7/−2.5/HNF-3mut., p3A7/−140/NF1mut., p3A7/−2.5/NF1mut., p3A7/−140/USFmut., p3A7/−2.5/USFmut., p3A7/−140/BTEmut., and p3A7/−2.5/BTEmut. were produced by site-directed mutagenesis using 3A4–140/−120-S, 3A4–140/−120-AS, 3A7NF1mut.-S, 3A7NF1mut.-AS, 3A7USFmut.-S, 3A7USFmut.-AS, 3A7/4BTEmut.-S, or 3A7/4BTEmut.-AS as mutated primers. To produce reporter plasmids p3A7E/−2.0, p3A7E/−360, p3A7E/−62, and p3A7E/−35, PCR was performed using 3A7–2.5 *Xho*I as a sense primer and 3A7/4–2.25 *Xho*I as an antisense primer. Synthesized fragments were digested with *Xho*I and then inserted into the *Xho*I site of p3A7/−2.0, p3A7/−360, p3A7/−62, and p3A7/−35.

Expression plasmids pPacSp1 (33) and pPacUSp3 (34), were generous gifts from Dr. Robert Tjian (University of California at Berkeley, Berkeley, CA) and Dr. Guntram Susuke (Institute fur Molekülarbiologie und Tumorforschung, Marburg, Germany), respectively. To construct an expression plasmid for HNF-3β (named pAcHNF-3β), HNF-3β cDNA was isolated from CMV-HNF-3β (35), a generous gift from Dr. Robert H Costa (University of Illinois, Chicago, IL) by *Spe*I/*Eco*RV digestion and was inserted into the *Eco*RV site of pAc5.1/V5-His (Invitrogen, Groningen, The Netherlands). To construct an expression plasmid for USF1 (named pAcUSF1), USF1 cDNA was isolated from USF-SRα (36) by *Xho*I/*Xba*I digestion and was inserted into the *Xho*I/*Xba*I site of pAc5.1/V5-His. To construct the HNF-3β expression plasmid (named pCI-HNF-3β) for *in vitro* transcription and translation, HNF-3β cDNA was isolated from CMV-HNF-3β by *Spe*I/*Eco*RV digestion and was inserted into the *Sma*I site of pCI-Neo carrying T7 promoter (Promega, Madison, WI).

Transient Transfection and Dual-Luciferase Assay—HepG2 cells (2×10^6 cells) were plated onto a 60-mm dish and then transfected with a reporter plasmid (2–8 μg) and pRL-SV40 (0.1 μg) (Promega) as an internal control by using the methods of calcium phosphate co-precipitation (37). Four hours after the DNA transfection, the cells were treated with 20% glycerol for 1.5 min. Transfection of DNA into SL2 cells was performed as described previously by Kudo (38). After 36 h, the cells were washed with phosphate-buffered saline, followed by a dual-luciferase assay according to the manufacturer's instructions (Promega).

In Vitro Transcription and Translation—*In vitro* transcription and translation assays were carried out using a rabbit reticulocyte lysate system (Toyoinki, Tokyo, Japan). Briefly, the pCI-HNF-3β expression plasmid under control of T7 promoter (1 μg) was added to a reaction mixture (50 μl) containing 50% of a rabbit reticulocyte lysate, 20 μM complete amino acid mixture, a ribonuclease inhibitor (40 units), and T7 RNA polymerase (20 units). The reaction mixture was incubated at 30 °C for 90 min. The reaction mixture (4 μl) was subjected to a gel shift assay.

Gel Shift Assay—Nuclear extracts were prepared from HepG2 cells according to the method of Dignam *et al*. (39). The gel shift assay was performed with double-stranded synthetic oligonucleotides labeled with [γ-^{32}P]ATP (Amersham Pharmacia Biotech) and T4 polynucleotide kinase (Takara). The binding reaction was carried out with a reaction mixture (10 μl) containing 25 mM Hepes (pH 7.9), 4% Ficoll, 40 mM KCl, 0.5 mM dithiothreitol, 0.1 mM EGTA, 1 mM $MgCl_2$, 5% glycerol, poly(dI-dC) (0.5 μg), nuclear extracts (10 μg), and a ^{32}P-labeled probe DNA (5 fmol). The mixture was incubated at 24 °C for 30 min. The samples were resolved on a 4% nondenaturing polyacrylamide gel in 0.5× Tris-boric acid-EDTA disodium salt at 100 V at room temperature and visualized by BAS-2500 Imaging Analyzer (Fuji Film, Tokyo, Japan). Antibodies to Sp1, Sp3, NF-κB p50, and USF1 were purchased from Santa Cruz Biotechnology (Santa Cruz, CA). Antibodies to HNF-3 (35) and NF1 were kindly provided by Dr. Robert H. Costa (University of Illinois, Chicago, IL) and Dr. Naoko Tanese (New York University, New York, NY), respectively. The supershift assay was performed using these antibodies as follows. After incubation of probe DNAs with nuclear extracts as described above, the antibodies were added to the reaction mixture and incubated at 24 °C for 1 h. The products were then analyzed by a gel shift assay. The sequence of oligonucleotides used as probes is as follows: 3A7NF-κB, 5′-CAGCTCTCAGTAGGCAAGTCCCTACATGTT-3′; 3A4NF-κB, 5′-CAGCTCTCAGTAGTCAAGTCCCTACATGTT-3′; 3A7NF-κBmut., 5′-CAGCTCTCAGTAGGAAAGTCCCTACATGTT-3′; Igκ, 5′-CAACAGAGGGGACTTTCCGAGGCCATCTG-3′; interleukin 2, 5′-CTAACAAAGAGGGATTTCACCTACAT-3′; H2k, 5′-CAGGGCTGGGGATTCCCCATCTCCACAGG-3′; SV40 core C, 5′-GTTAGGGTGTGGAAAGTCCCCAGGCTC-3′; acute phase response element, 5′-CCACAGTTGGGATTTCCCAACCTGACCAGA-3′; Sp1, 5′-ATTCGAT CGGGGCGGGGCGAGC-3′; C/EBP, 5′-TGCAGATTGCGCAATCTGCA-3′; 3A7–136/−99, 5′-GTGTGTGATTATTTGCCAACTGCCAACTGCCGAGGTGGAGAAGCCTC-3′; 3A4–139/−102, 5′-GTGTGTGATTCTTTGCCAACTTCCAAGGTGGAGAAGCCTC-3′; 3A7–136/−117, 5′-TGTGTGATTATTTGCCAACT-3′; 3A4–139/−120, 5′-TGTGTGATTCTTTGCCAACT-3′; 3A7–119/−100, 5′-ACTGCCGAGGTGGAGAAGCC-3′; 3A4–122/−103, 5′-ACTTCCAAGGTGGAGAAGCC-3′; 3A7–103/−80, 5′-AGCCTCTTCCGACTGCAGGCAGAG-3′; 3A4–106/−83, 5′-AGCCTCTTCCAACTGCAGGCAGAG-3′; 3A7–90/−63, 5′-CTGCAGGCAGAGCACGGGGGCCCTGCTAC-3′; 3A4–93/−65, 5′-CTGCAGGCAGAGCACAGGTGGCCCTGCTAC-3′; HNF-3, 5′-TCTGATTATTGACTTAGTCAAG-3′; NF1, 5′-TATTTTGGATTGAAGCCAATATGATA-3′; 3A7NF1mut., 5′-TGTGTCATTATTTGCGAACT-3′; 3A4NF1mut., 5′-TGTGTCATTCTTTGCGAACT-3′; 3A7USFmut., 5′-CTGCAGGCAGAGCATAAGGGCCCTGCTAC-3′; adenovirus major late promoter, 5′-GATCCGTAGGCCACGTGACCCGGG-3′; 3A7/4BTE, 5′-CTCCAGCCCTGCCTCCTT CT-3′; and 3A7/4BTEmut., 5′-CTCCAGCGAGGCCTCCTTCT-3′.

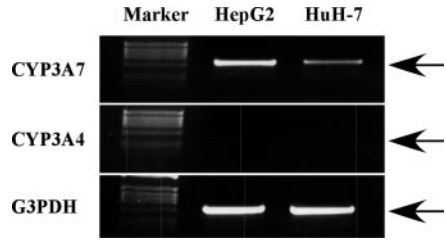

FIG. 1. **RT-PCR for analyzing the expression of CYP3A7 and CYP3A4 mRNAs in human hepatoma cells.** PCR was performed for 30 cycles with total RNAs (1 μg) prepared from HepG2 and HuH-7 cells. The expression of glyceraldehyde-3-phosphate dehydrogenase was also determined as an internal control. The positions of the expected sizes of PCR products are indicated by *arrows*.

RESULTS

Transcriptional Activities of the CYP3A7 and CYP3A4 Genes in Human Hepatoma Cells—The expression levels of CYP3A7 and CYP3A4 mRNAs in HepG2 or HuH-7 cells were determined by RT-PCR. CYP3A7 but not CYP3A4 mRNA was detectable in both hepatoma cells (Fig. 1). Because the specific expression of CYP3A7 mRNA in HepG2 or HuH-7 cells was in accordance with that seen in human fetal livers (18), these cells seem to be a useful *in vitro* model to analyze the function of the promoter of the *CYP3A7* gene expressed in human fetal livers.

To identify a possible *cis*-acting element(s) specifically responsible for the transcriptional regulation of the *CYP3A7* gene, HepG2 cells were transiently transfected with a series of 5′-truncated promoter-luciferase chimeric genes as shown in Fig. 2. A reporter plasmid p3A7/−5.5 contained a region from nucleotides −5564 to +105 of the *CYP3A7* gene, whereas a reporter plasmid p3A4/−5.5 had a region from nucleotides −5551 to +103 of the *CYP3A4* gene. Luciferase activity seen with p3A7/−5.5 was 28-fold higher than that seen with p3A4/−5.5 (Fig. 2), although 5′-flanking regions up to −5.5 kb were 90% identical between the *CYP3A7* and *CYP3A4* genes (data not shown). This result indicates that a possible enhancer(s) is present specifically in the region from −5.5 kb to +105 of the *CYP3A7* gene. To further clarify the region involved in the transcription of the gene, the 5′-flanking sequence of the *CYP3A7* or *CYP3A4* gene was successively deleted. The deletion constructs were then transfected into HepG2 cells. Deletion to −2.5 kb of the *CYP3A7* gene increased the luciferase activity by 1.8-fold as compared with the level seen with p3A7/−5.5. Thus, a negative regulatory element(s) was assumed to be present in the region from −3.0 to −2.5 kb. Deletion to −2.0 kb decreased the luciferase activity to 18% of the level seen with p3A7/−2.5. Although the luciferase activity with p3A7/

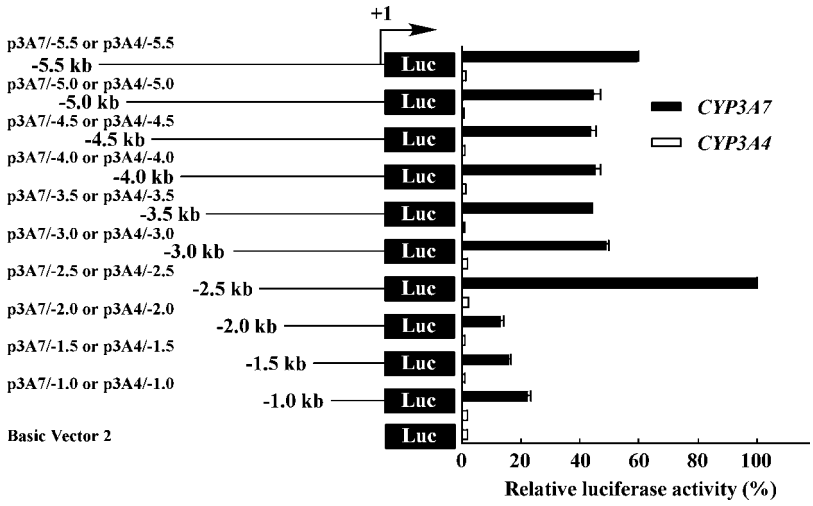

FIG. 2. **Transcriptional activity of the 5′-flanking region of the *CYP3A7* and *CYP3A4* genes in HepG2 cells.** The construction of deletion mutants is described under "Experimental Procedures." HepG2 cells (2×10^6 cells) were transiently transfected by the calcium phosphate co-precipitation method (37) with a reporter plasmid (8 μg). The cells were harvested 36 h after DNA transfection, and luciferase activity was assayed. The numbers given to the deletion mutants indicate the 5′-end of the 5′-flanking sequence of the *CYP3A7* or *CYP3A4* gene counted negatively from the transcriptional start site (22, 23). The luciferase activity represents the average ± S.D. from at least three independent experiments. The mean value obtained with p3A7/−2.5 was defined as 100%.

−1.0 was one-fifth of that with p3A7/−2.5, the luciferase activity was still 10-fold higher than that with p3A4/−1.0 or Basic Vector 2. These data indicate that positive regulatory elements locate in the regions from −2.5 to −2.0 kb and from −1.0 kb to +105 of the *CYP3A7* gene.

Identification of the Upstream Enhancer of the CYP3A7 Gene—A second set of successive deletion mutants was transfected into HepG2 cells as shown in Fig. 3*A*. Although deletion of the region from −2.50 to −2.35 kb of the *CYP3A7* gene decreased the luciferase activity to 80% of the level seen with p3A7/−2.5 containing the region up to −2.50 kb of the *CYP3A7* gene, further deletion to −2.30 kb lowered the luciferase activity to 18% of the level seen with p3A7/−2.5. The result indicates that the region from −2.35 to −2.30 kb of the *CYP3A7* gene functions as an enhancer. The sequence of the 5′-flanking region from −2.35 to −2.30 kb of the *CYP3A7* gene was found to contain a 1-base pair mismatch as compared with that of the corresponding region of the *CYP3A4* gene, namely guanine base for the *CYP3A7* gene and thymine base for the *CYP3A4* gene (Fig. 3*B*). To examine whether or not the 1-base pair mismatch between the *CYP3A7* and *CYP3A4* genes causes difference in transcriptional activity, the nucleotide sequence was changed from a guanine base at position −2313 of the *CYP3A7* gene to a thymine base and conversely from thymine base at position −2318 of the *CYP3A4* gene to guanine base by site-directed mutagenesis (Fig. 3*C*). The intact or the mutant 5′-flanking region from −2.50 to −2.25 kb of the *CYP3A7* or *CYP3A4* gene was then linked to the *CYP3A7* minimal promoter (−62/+105) possessing BTE and TATA box. Reporter plasmids p3A7Ewild and p3A4Ewild possessed the intact *CYP3A* genes, whereas reporter plasmids p3A7Emut. and p3A4Emut. had the mutated *CYP3A* genes. As shown in Fig. 3*C*, the luciferase activity with p3A7Ewild was ~5-fold higher than that with p3A4Ewild. Luciferase activity with p3A7Emut. was one-fifth the level seen with p3A7Ewild. On the other hand, the luciferase activity with p3A4Emut. was 6-fold higher than that with p3A4Ewild. These results indicate that the 1-base pair mismatch leads to the difference in enhancer activity between the *CYP3A7* and *CYP3A4* genes. Comparing the nucleotide sequence from −2.35 to −2.30 kb of the *CYP3A7* gene with the elements reported so far, we found that the sequence of the region containing the 1-base pair mismatch partially overlapped with those of NF-κB-binding sites (Fig. 3*D*). The sequence of the NF-κB-like elements of the *CYP3A7* and *CYP3A4* genes had 1- and 2-base pair changes, respectively, as compared with the most typical NF-κB-binding sequence found in the Igκ gene (40) and SV40 core C (41). To compare the enhancer activity of the NF-κB-like elements between the *CYP3A7* and *CYP3A4* genes, two copies of the NF-κB-like element of the *CYP3A7* or *CYP3A4* gene were linked to the *CYP3A7* minimal promoter containing a region from nucleotides −62 to +105 (Fig. 3*E*). Luciferase activity with p3A7NF-κB was 5-fold higher than that with p3A4NF-κB, although p3A4NF-κB showed some enhancer activity as compared with p3A7/−62 carrying the minimal promoter. This result was consistent with the data shown in Fig. 3*C*, indicating that the NF-κB-like element of the *CYP3A7* gene was required for the transcriptional activation of the *CYP3A7* gene.

Sp1 and Sp3 as Possible Factors Binding to the NF-κB-like Element of the CYP3A7 Gene—Transcription factors capable of interacting with the NF-κB-like element of the *CYP3A7* or *CYP3A4* gene were investigated by a gel shift assay (Fig. 4*A*). Using nuclear extracts prepared from HepG2 cells, three shifted bands (complexes A, B, and C) appeared with the NF-κB-like element of the *CYP3A7* gene (defined this probe DNA as *CYP3A7* NF-κB-like element), whereas one shifted band (complex D) appeared with the NF-κB-like element of the *CYP3A4* gene (defined this probe DNA as *CYP3A4* NF-κB-like element). The three shifted bands (complexes A, B, and C) were not eliminated by the addition of a 100-fold molar excess of the *CYP3A4* NF-κB-like element, although the intensity of the shifted band A was weakened. On the other hand, the shifted band D was abolished by the addition of the *CYP3A7* or *CYP3A4* NF-κB-like element. Thus, the shifted band A, which appeared with the *CYP3A7* NF-κB-like element, is likely to be partially overlapped with the shifted band D. These results indicate that the three complexes A, B, and C, but not D, are complexes that bind specifically to the *CYP3A7* NF-κB-like element. To identify a constitutive factor(s) bound to the *CYP3A7* NF-κB-like element, we carried out a gel shift assay using competitors having NF-κB sequences found in the Igκ (40), interleukin 2 (42), major histocompatibility complex H2K (43), angiotensinogen (44) genes, and SV40 core C (41) (Fig. 4*B*). We also employed competitors having Sp1 and C/EBP consensus sequences, because Sp1 and C/EBP were reported to bind to a subset of NF-κB-binding sites (44, 45). The formation of the three complexes, A, B, and C, was partially inhibited by the NF-κB sequences of the Igκ, interleukin 2, H2k, angiotensinogen genes, and SV40 core C. The addition of Sp1 consensus sequence strongly inhibited the formation of all of the three complexes, A, B, and C. A faint band, which was not competed out by the Sp1 consensus sequence (Fig. 4*B*), is likely to be complex D. To examine the binding specificity of the Sp family, a gel shift assay was performed using an Sp1 consensus site as a probe and the NF-κB-like element of the *CYP3A7* or *CYP3A4* gene as a competitor (Fig. 4*C*). The binding of the Sp

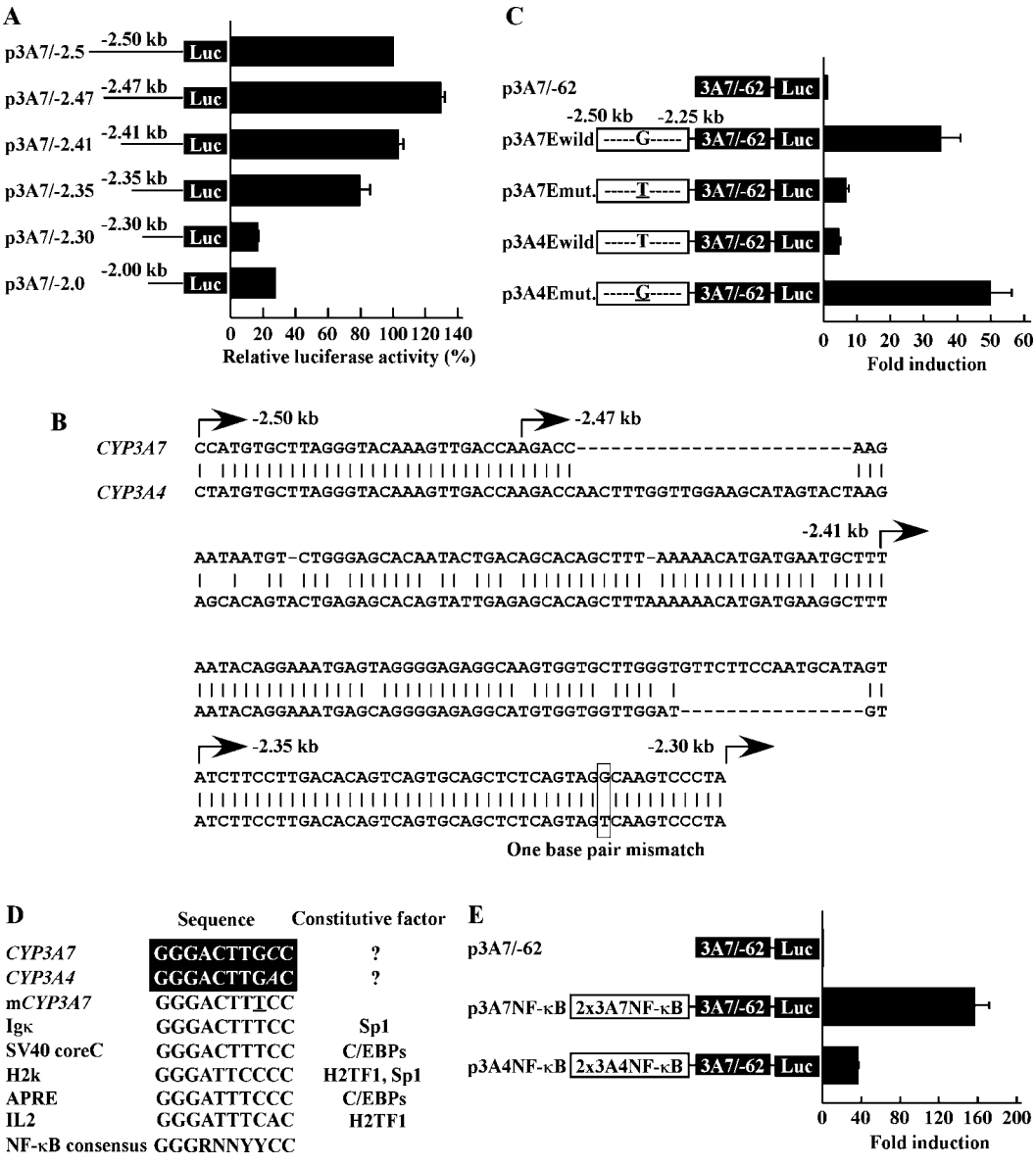

FIG. 3. **Identification and characterization of an NF-κB-like enhancer in the *CYP3A7* gene.** *A*, transcriptional activity of the region from −2.5 to −2.0 kb of the *CYP3A7* gene in HepG2 cells. The activity represents the average ± S.D. from at least three independent experiments. The mean value obtained with p3A7/−2.5 was defined as 100%. *B*, nucleotide sequences from −2.5 to −2.3 kb of the *CYP3A7* and *CYP3A4* genes. The *arrows* indicate the 5′-end of the 5′-flanking sequence of the *CYP3A7* gene in deletion constructs, p3A7/−2.5, p3A7/−2.47, p3A7/−2.41, p3A7/−2.35, and p3A7/−2.30. The 1-base pair mismatch (G/T) between the two genes in the *CYP3A7* enhancer region is indicated by a *box*. *C*, effects of the 1-base pair substitution between the *CYP3A7* and *CYP3A4* genes on an enhancer activity in HepG2 cells. The construction of reporter plasmids is described under "Experimental Procedures." HepG2 cells (2×10^6 cells) were transiently transfected with a reporter plasmid (2 μg), p3A7/−62, p3A7Ewild, p3A7Emut., p3A4Ewild, and p3A4Emut. The mutated sequence is *underlined*. The data are presented as a −fold induction relative to the activity with p3A7/−62. The activities represent the averages ± S.D. from at least three independent experiments. *D*, alignment of the NF-κB-binding sites conserved in the *CYP3A7* and other genes. The sequences are aligned with decameric nucleotides, GGGRNNYCC, known to be a consensus binding motif for NF-κB (89, 90). The *right column* indicates the constitutive factors bound to each sequence. The mutated sequence is *underlined*. An *italic letter* indicates a different nucleotide sequence between the *CYP3A7* and *CYP3A4* genes. *E*, enhancer activity of the NF-κB-like element in the *CYP3A7* or *CYP3A4* gene in HepG2 cells. The construction of reporter plasmids is described under "Experimental Procedures." HepG2 cells (2×10^6 cells) were transiently transfected with a reporter plasmid (2 μg), p3A7/−62, p3A7NF-κB, and p3A4NF-κB. The results are presented as fold induction relative to the activity with p3A7/−62, and the values represent the averages ± S.D. from at least three independent experiments.

family to the most typical Sp1 consensus sequence was inhibited by increasing the amounts of the *CYP3A7* NF-κB-like element added, whereas the addition of the *CYP3A4* NF-κB-like element was ineffective. Thus, it appeared that constitutive factors specifically bound to the *CYP3A7* NF-κB-like element were Sp family members. To further confirm the binding of the Sp family to the *CYP3A7* NF-κB-like element, a supershift assay using antibodies to Sp1 and Sp3, which are abundant forms of the Sp family in various types of cells (46), was performed. Antibodies to the p50 subunit of NF-κB complex were also used because the p50 homodimer but not p50/p65 heterodimer is reported to be retained in the nuclei without stimuli (47). As shown in Fig. 4*D*, antibodies to Sp1 and Sp3 supershifted complex A and complexes B and C, respectively. Complex D was not affected by antibodies to Sp1, Sp3, or the p50 subunit of NF-κB complex. These results indicate that both Sp1 and Sp3 bind to the *CYP3A7* NF-κB-like element but not to the *CYP3A4* NF-κB-like element.

Transactivation of the Promoter of the CYP3A7 Gene by Sp1 and Sp3 through the NF-κB-like Element—To determine the

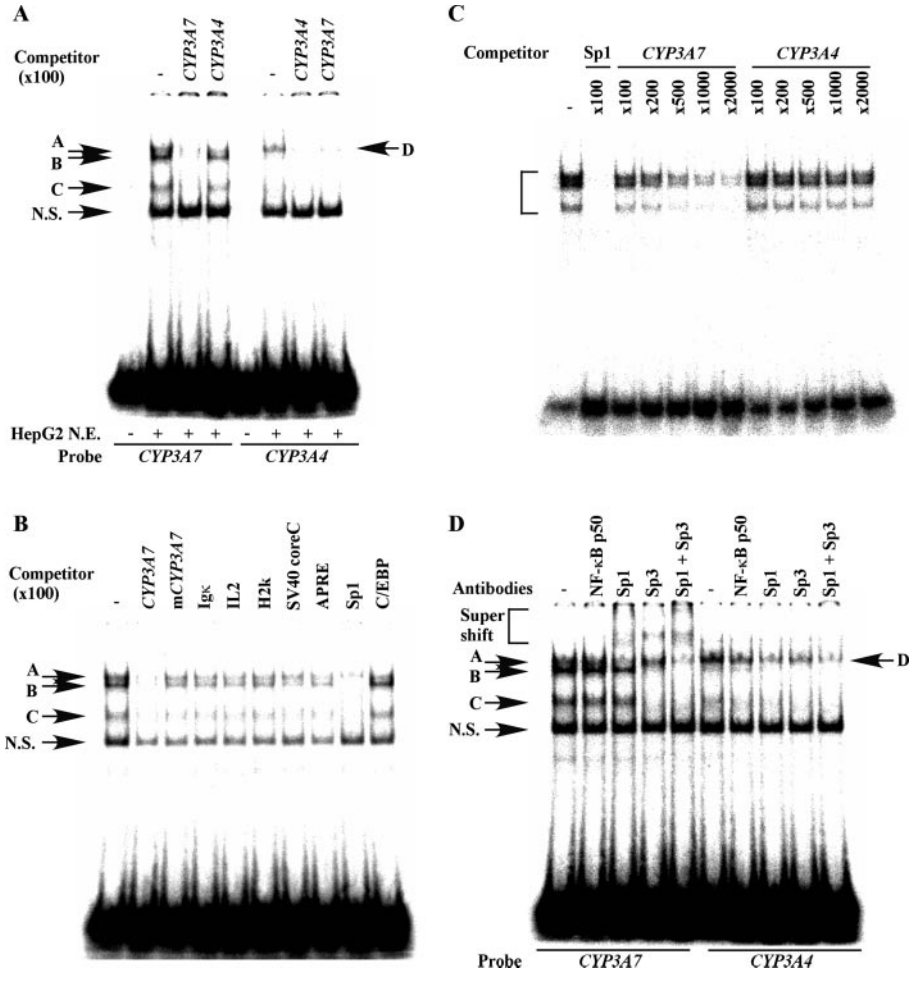

FIG. 4. **Interaction of Sp1 and Sp3 with the *CYP3A7* NF-κB-like element.** *A*, gel shift assay with the NF-κB-like elements in the *CYP3A7* and *CYP3A4* genes. Nuclear extracts (10 μg) from HepG2 cells were incubated with the ^{32}P-labeled NF-κB-like elements of the *CYP3A7* and *CYP3A4* genes. Competition analysis was carried out by the addition of a 100-fold molar excess of the unlabeled *CYP3A7* or *CYP3A4* NF-κB-like element. DNA-binding complex was resolved by a 4% polyacrylamide gel. The *arrows* indicate the specific complexes A, B, C, and D. *N.S.*, nonspecific band; *N.E.*, nuclear extracts. *B*, effects of various competitors on the binding of nuclear factors to the *CYP3A7* NF-κB-like element. Nuclear extracts (10 μg) from HepG2 cells were incubated with the ^{32}P-labeled *CYP3A7* NF-κB-like element in the presence of a 100-fold molar excess of various competitors. *C*, effects of the *CYP3A7* and *CYP3A4* NF-κB-like elements on the binding of nuclear factors to an Sp1 consensus sequence. Nuclear extracts (10 μg) from HepG2 cells were incubated with the ^{32}P-labeled Sp1 consensus sequence in the presence of 100–2000-fold molar excess of the unlabeled Sp1 consensus sequence, the NF-κB-like element of the *CYP3A7* or *CYP3A4* gene. The region of DNA-binding complexes is indicated by *bracket*. *D*, supershift assay using antibodies to Sp1, Sp3, or NF-κB p50. The ^{32}P-labeled NF-κB-like element of the *CYP3A7* or *CYP3A4* gene was incubated with nuclear extracts (10 μg) prepared from HepG2 cells in the presence of antibodies (1 μl) to Sp1, Sp3, or NF-κB p50. The supershifted bands are indicated by the *bracket*.

relative contribution of each Sp isoform to the *CYP3A7* enhancer activity, *Drosophila* SL2 cells that lacked an endogenous Sp family (33) were transiently transfected with a reporter plasmid, p3A7/−62, p3A7NF-κB, or p3A4NF-κB, together with an Sp1 or Sp3 expression plasmid (Fig. 5). The levels of basal transcriptional activities of p3A7/−62, p3A7NF-κB, and p3A4NF-κB in *Drosophila* SL2 cells were nearly the same (data not shown). The transcriptional activities of the p3A7/−62 and p3A4NF-κB were slightly increased by Sp1 or Sp3, whereas the transcriptional activity of p3A7NF-κB was increased ~20-fold when an Sp expression plasmid, pPacSp1 (0.1 μg) or pPacUSp3 (0.1 μg), was co-transfected into SL2 cells in combination with p3A7NF-κB. These results indicate that both Sp1 and Sp3 act as the activators of the *CYP3A7* gene through the NF-κB-like element identified in the present study.

Identification of the Proximal Promoter of the CYP3A7 Gene—A proximal promoter region from −1.0 kb to +105 of the *CYP3A7* gene also showed higher luciferase activity than did that of the *CYP3A4* gene (Fig. 2). To identify a possible regulatory element(s) in the proximal promoter of the *CYP3A7* gene, the sequences of the *CYP3A7* and *CYP3A4* genes were successively deleted as shown in Fig. 6*A*. The maximal luciferase activity was seen with the p3A7/−140 reporter plasmid. The luciferase activity with the p3A7/−140 was 5-fold higher than that with the p3A4/−140 harboring the corresponding region of the *CYP3A4* gene. Deletion to −90 decreased the luciferase activity to 50% of the level seen with the p3A7/−140, although the luciferase activity was still higher than that with the p3A4/−90. Further deletion to −62 of the *CYP3A7* gene

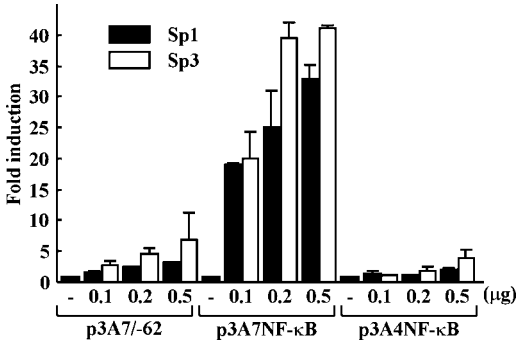

FIG. 5. **Activation by Sp1 and Sp3 of the *CYP3A7* gene in *Drosophila* SL2 cells.** A reporter plasmid (2 μg), p3A7/−62, p3A7NF-κB, or p3A4NF-κB was co-transfected into SL2 cells (1×10^6 cells) with increasing amounts of expression plasmids for Sp1 (*closed bars*) or Sp3 (*open bars*). The cells were harvested 36 h after transfection, and the luciferase activity was assayed. The results are expressed as fold induction relative to the activity obtained by co-transfection with the expression vector pPac as a control. The activity represents the average ± S.D. from at least three independent experiments.

attenuated the luciferase activity to 10% of the level seen with the p3A7/−140. These results indicate that the region from nucleotides −140 to −62 is also a necessary region for the transcriptional activation of the *CYP3A7* gene.

To compare the binding pattern of transcription factors, the proximal promoter region of the *CYP3A7* gene was cut to yield five DNA fragments: −136/−99, −136/−117, −119/−100, −103/−80, and −90/−63 (Fig. 6*B*). The proximal promoter region of the *CYP3A4* gene was also divided into the corresponding DNA fragments: −139/−102, −139/−120, −122/

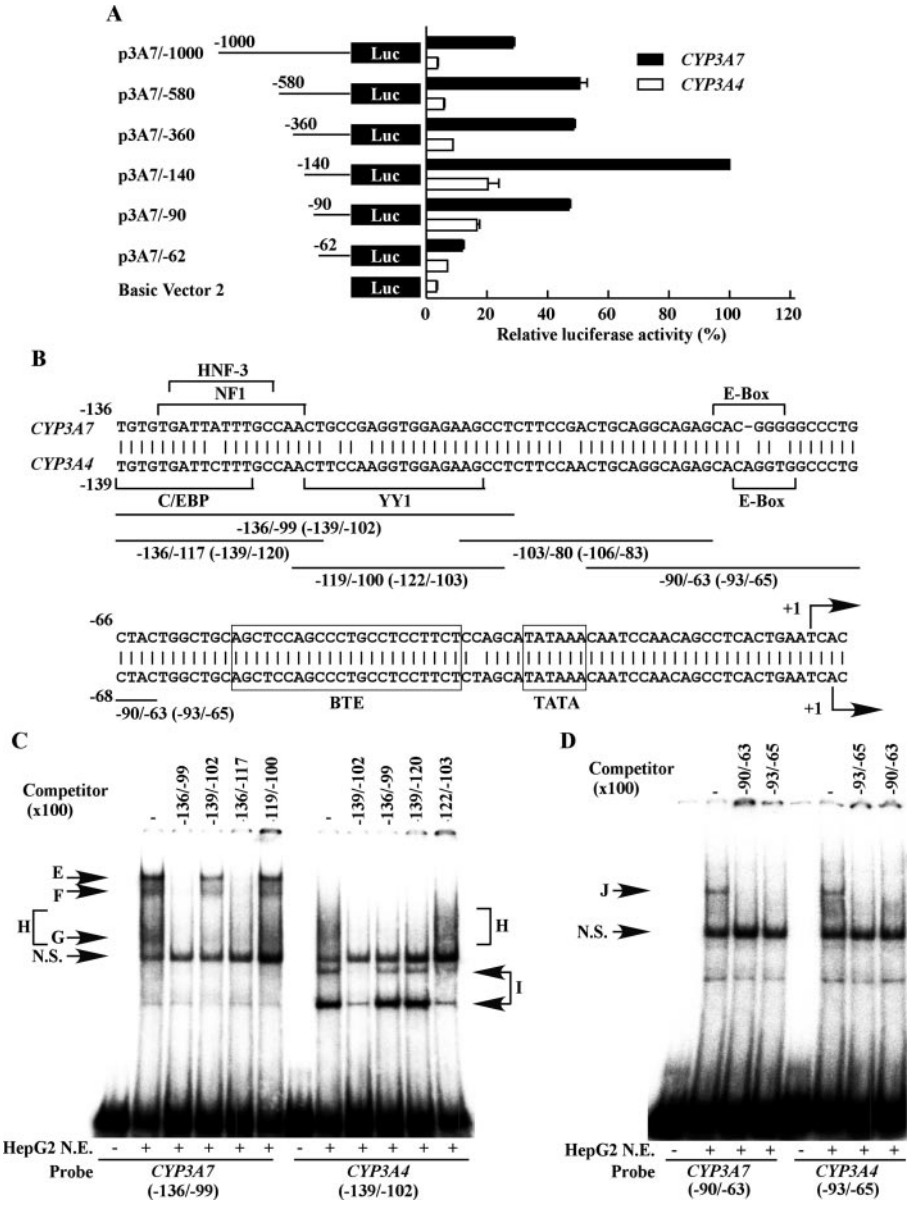

FIG. 6. **Characterization of the proximal promoter of the *CYP3A7* gene in HepG2 cells.** *A*, deletion analysis of a region from −1.0 kb to +105 of the *CYP3A7* gene in HepG2 cells. The construction of deletion mutants is described under "Experimental Procedures." The *numbers* given to deletion mutants indicate the 5′-end of the 5′-flanking sequence of the *CYP3A7* or *CYP3A4* gene counted negatively from the transcriptional start site. The activity represents the average ± S.D. from at least three independent experiments. The mean value obtained with p3A7/−140 was defined as 100%. *B*, nucleotide sequences between nucleotides −136 and +3 of the *CYP3A7* and *CYP3A4* genes. The transcription start sites of the *CYP3A7* and *CYP3A4* genes (22, 23) are assigned as +1 shown by *arrows*. BTE and TATA box are *boxed*. Putative *cis*-acting elements are indicated by *brackets*. Fragments used for gel shift assay, *e.g.* −136/−99 for the *CYP3A7* gene and (−139/−102) for the *CYP3A4* gene, are *underlined*. *C*, gel shift assay with the −136/−99 and −139/−102 fragments of the respective *CYP3A7* and *CYP3A4* genes. Nuclear extracts (10 μg) from HepG2 cells were incubated with the ^{32}P-labeled −136/−99 or −139/−102 fragment in the presence of a 100-fold molar excess of a competitor. DNA-binding complexes are shown by *arrows*. *N.S.*, nonspecific band; *N.E.*, nuclear extracts. *D*, gel shift assay with the −90/−63 and −93/−65 fragments of the respective *CYP3A7* and *CYP3A4* genes. Nuclear extracts (10 μg) from HepG2 cells were incubated with the ^{32}P-labeled −90/−63 or −93/−65 fragment in the presence of a 100-fold molar excess of a competitor. DNA-binding complexes (G, H, I, and L) are shown by *arrows*. *N.S.*, nonspecific band; *N.E.*, nuclear extracts.

−103, −106/−83, and −93/−65 (Fig. 6*B*). These fragments were then used as probes or competitors for a gel shift assay. As can be seen in Fig. 6*C*, different DNA-binding complexes (complexes E, F, and G for *CYP3A7* and complex I for *CYP3A4*) appeared with the −136/−99 fragment of the *CYP3A7* and the −139/−102 fragment of the *CYP3A4*, whereas a broad and faint complex H was detected with the fragments of both genes. Complexes E, F, G, and H were decreased by the addition of the −136/−117 fragment of the *CYP3A7* gene, whereas complex I was diminished by the −122/−103 fragment of the *CYP3A4* gene. As shown in Fig. 6*D*, a complex J appeared with both the −90/−63 fragment of the *CYP3A7* and the −93/−65 fragment of the *CYP3A4* genes. No DNA-binding complexes appeared with the −103/−80 and −106/−83 fragments (data no shown). Searching for a possible binding site(s) of reported transcription factor, we found that the putative binding sites for liver-enriched transcription factors (HNF-3, C/EBP, and NF1), transcription repressor YY1, and the E-box-like elements were located within the −136/−117, −119/−100, and −90/−63 fragments, respectively (Fig. 6*B*).

HNF-3β, NF1, USF1, and Sp1/Sp3 as Proteins Binding to the Proximal Promoter Region of the CYP3A7 Gene—To identify the factors detected with the −136/−99 fragment of the *CYP3A7* gene, a gel shift assay using the −136/−117 fragment of the *CYP3A7* gene and the −139/−120 fragment of the *CYP3A4* gene as a probe and nuclear extracts prepared from HepG2 cells was performed (Fig. 7*A*). In accordance with the data shown in Fig. 6*C*, DNA-binding complexes E, F, and G appeared with the −136/−117 fragment of the *CYP3A7* gene as a probe. Complex H was detected with the same migration with the −136/−117 and −139/−120 fragments of both the *CYP3A7* and *CYP3A4* genes. To further characterize a nuclear factor(s) binding to the *CYP3A7* proximal promoter, a gel shift assay was performed using mutated probe, NF1mut., and various possible competitors, HNF-3, NF1, and C/EBP (Fig. 7*B*). As shown in Fig. 7*C*, NF1mut. was designed to have two mutations in the NF1-binding site of the *CYP3A7* and *CYP3A4* genes. Three shifted bands (E, F, and G) present in the −136/−117 of the *CYP3A7* gene disappeared in the presence of HNF-3. Supporting this result, the binding of nuclear factors to HNF-3 was also diminished by the addition of the −136/−117 fragment of the *CYP3A7* gene. The result indicates that HNF-3 or an HNF-3-related factor(s) interacts with the −136/−117 fragment of the *CYP3A7* gene. Complex H seen with the −136/

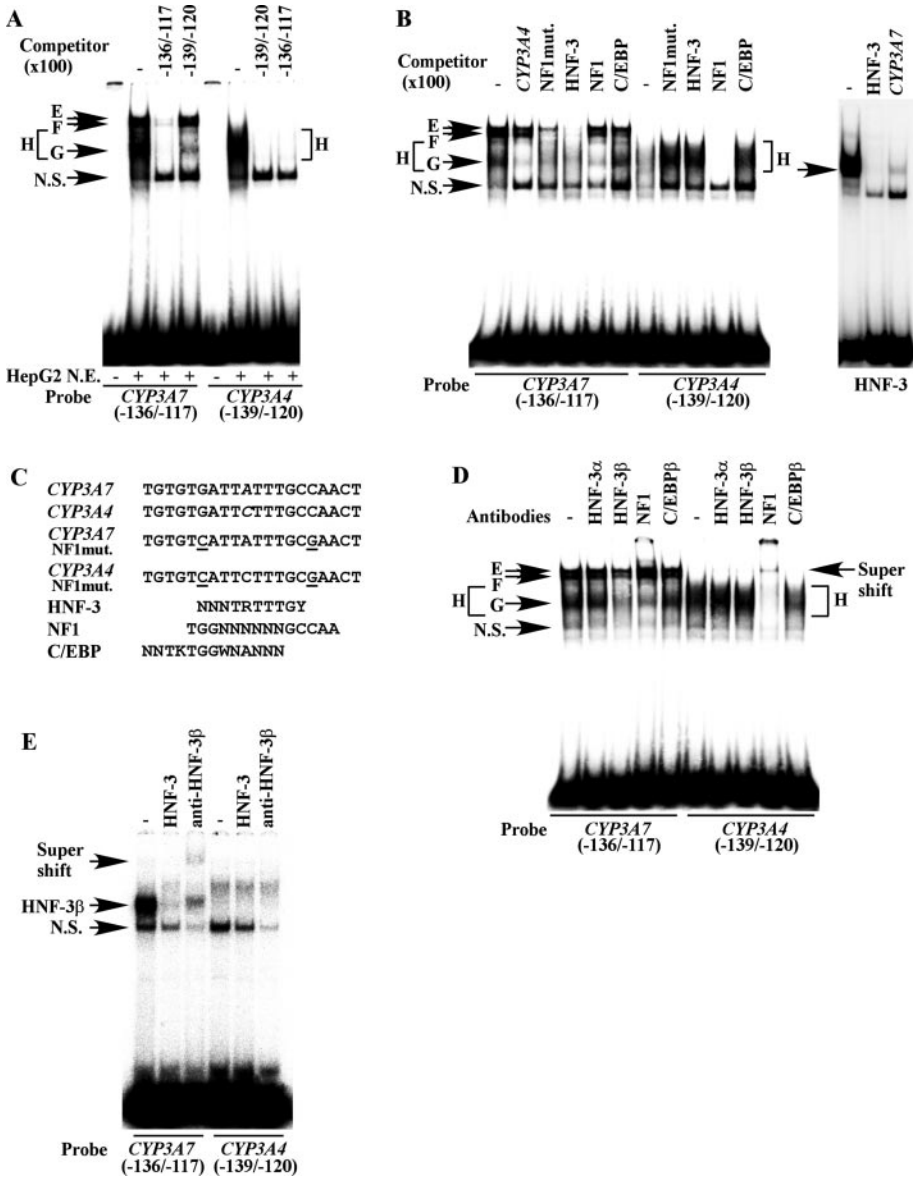

FIG. 7. **The binding of nuclear factors to the −136/−117 fragment of the *CYP3A7* gene in HepG2 cells.** *A*, gel shift assay with the −136/−117 and −139/−120 fragments of the respective *CYP3A7* and *CYP3A4* genes. Nuclear extracts (10 μg) from HepG2 cells were incubated with the ^{32}P-labeled −136/−117 or −139/−120 fragment. Competition analysis was carried out by the addition of a 100-fold molar excess of unlabeled −136/−117 and −139/−120 fragments of the *CYP3A7* and *CYP3A4* genes, respectively. The *arrows* indicate the DNA-binding complexes. *N.S.*, nonspecific band; *N.E.*, nuclear extracts. *B*, effects of various competitors on the binding of nuclear factors to the −136/−117 or −139/−120 fragment. Nuclear extracts (10 μg) from HepG2 cells were incubated with the ^{32}P-labeled −136/−117, −139/−120, or HNF-3 in the presence of a 100-fold molar excess of a competitor. DNA-binding complexes are indicated by *arrows*. *C*, oligonucleotides used for gel shift assays. An *italic letter* indicates a nucleotide change between the −136/−117 of the *CYP3A7* gene and the −139/−120 fragment of the *CYP3A4* gene. Changed nucleotides in mutant probes are *underlined*. Consensus binding sequences for HNF-3, NF1 or C/EBP (from TFSEARCH, pdap1.trc.rwcp.or.jp/research/db/TFSEARCH.html) are aligned with the −136/−117 and −139/−120 fragments of the respective *CYP3A7* and *CYP3A4* genes. *D*, supershift assay with antibodies to HNF-3α, HNF-3β, NF1, or C/EBPβ. ^{32}P-Labeled −136/−117 or −139/−120 fragment was incubated with nuclear extracts (10 μg) from HepG2 cells in the presence or absence of antibodies (1 μl) to HNF-3α, HNF-3β, NF1, or C/EBPβ. Supershifted bands are shown by *arrows*. *E*, gel shift assay with *in vitro* synthesized HNF-3β proteins. ^{32}P-Labeled −136/−117 and −139/−120 fragments of the respective *CYP3A7* and *CYP3A4* genes were incubated with HNF-3β proteins produced by *in vitro* transcription and translation in the presence or absence of a competitor HNF-3 or antibodies to HNF-3β (anti-HNF-3β).

−117 and −139/−120 fragments of the *CYP3A7* and *CYP3A4* genes disappeared in the presence of NF1. The addition of NF1mut., HNF-3, or C/EBP was ineffective. This result was in agreement with the fact that the putative NF1-binding sequence was conserved in the proximal promoter region of the *CYP3A7* and *CYP3A4* genes (Fig. 7*C*). To confirm the binding of HNF-3 and NF1 to the −136/−117 fragment, a gel shift assay was performed using antibodies to HNF-3, NF1 or C/EBP (Fig. 7*D*). The formation of complex G was diminished by the addition of antibodies to HNF-3β, although complexes E and F were unaffected by the addition of antibodies to either HNF-3α or HNF-3β. To distinguish HNF-3β from NF1, antibodies to NF1 were used for a supershift assay. The formation of complex H decreased when antibodies to a N-terminal peptide conserved among NF1 isoforms were added to nuclear extracts prepared from HepG2 cells (Fig. 7*D*). Thus, complex H was confirmed to be derived from NF1. Because HNF-3- and NF1-binding sites in the promoter region of the *CYP3A7* gene perfectly overlapped, it seemed likely that HNF-3β and the members of the NF1 family bound to the HNF-3/NF1-binding site in a mutually exclusive manner. Detailed analysis of complex E and F is currently under investigation. To further confirm the specific binding of HNF-3β to the *CYP3A7* gene, the −136/−117 and −139/−120 fragments of the *CYP3A7* and *CYP3A4* genes were incubated with *in vitro* translated HNF-3β protein. As shown in Fig. 7*E*, HNF-3β bound to the −136/−117 fragment of the *CYP3A7* gene to generate a clear band. The binding of HNF-3β was competed out by an HNF-3 binding site and was inhibited by antibodies to HNF-3β. These results indicate that HNF-3β is a component of complex G.

We also confirmed that complex I seen with the −122/−103 fragment of the *CYP3A4* gene was identical to YY1 (data not shown). The functional role of YY1 in the transcriptional regulation of the *CYP3A4* gene will be described elsewhere.

E-box is reportedly a target element for several transcription factors belonging to a basic helix-loop-helix family (48). Among them, USF appears to be the most predominant basic helix-loop-helix factor in the liver (49). The E-box-like elements of the *CYP3A7* and *CYP3A4* genes resembled the USF-binding elements of the rat γ-fibrinogen gene (50) and the human β-globin locus control region (51), respectively (Fig. 8*A*). To examine whether the E-box-like element of the *CYP3A7* gene is indeed necessary for the formation of complex J, mutations were introduced into the E-box-like element of the −90/−63 fragment of the *CYP3A7* gene as shown in Fig. 8*A*. The formation of complex J with the −90/−63 fragment of the *CYP3A7* gene was not completely abolished by the addition of the mutated E-box, m*CYP3A7* (Fig. 8*B*). Additionally, the formation of complex J

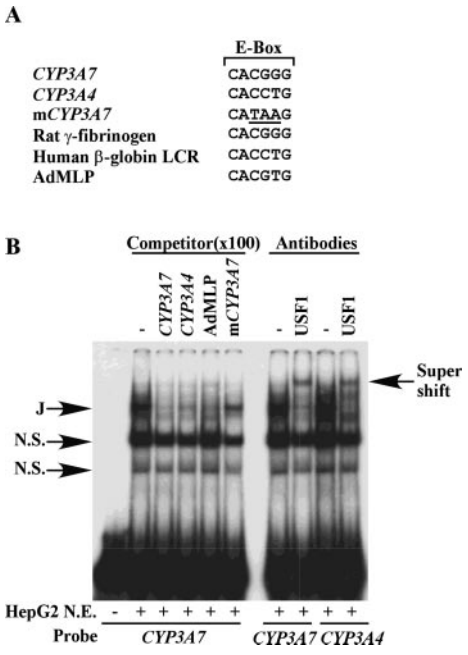

FIG. 8. **Interaction of USF1 with the E-box of the *CYP3A7* and *CYP3A4* genes in HepG2 cells.** *A*, alignment of the binding sites for USF1. The sequences are aligned with the 6-base pair domain CANNTG, which is a consensus binding motif for USF1 (48). Changed nucleotides in mutant oligonucleotide are *underlined*. *B*, gel shift assay with the −90/−63 and −93/−65 fragments of the *CYP3A7* and *CYP3A4* genes. ^{32}P-Labeled −90/−63 or −93/−65 fragment was incubated with nuclear extracts (10 μg) from HepG2 cells in the presence or absence of a competitor or antibodies (1 μl) to USF1. The DNA-binding complexes are shown by *arrow J*. *N.S.*, nonspecific band; *N.E.*, nuclear extracts.

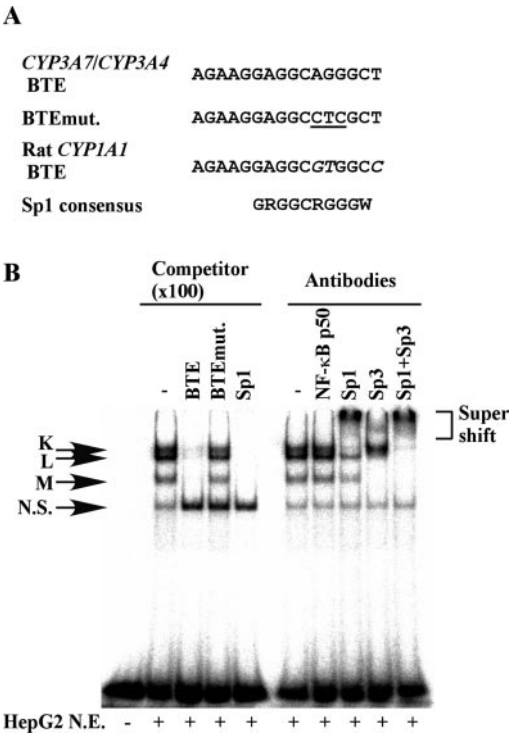

FIG. 9. **Nuclear factors binding to the BTE of the *CYP3A7* and *CYP3A4* genes.** *A*, alignment of the BTE of the *CYP3A7* or *CYP3A4* gene. The sequences of BTEs in the human *CYP3A* and the rat *CYP1A1* genes are aligned with a 10-base pair domain GRGGCRGGGW, which is a consensus binding motif for Sp1 (from TFSEARCH). Changed nucleotides in the mutant BTE are *underlined*. *Italic letters* represent nucleotide changes in BTEs of the human *CYP3A* and the rat *CYP1A1* genes. *B*, identification of a factor(s) binding to BTE. ^{32}P-Labeled BTE was incubated with nuclear extracts (10 μg) from HepG2 cells in the presence or absence of a competitor or antibodies (1 μl) to NF-κB p50, Sp1, or Sp3. The DNA-protein complexes are shown by *arrows*. *A bracket* indicates the supershifted band. *N.S.*, nonspecific band; *N.E.*, nuclear extracts.

was inhibited by the addition of a fragment having the USF-binding sequence of the adenovirus major late promoter (52) (Fig. 8*B*). As expected, complex J was supershifted by antibodies against USF1 when the E-boxes of the *CYP3A7* and *CYP3A4* genes were used as probes (Fig. 8*B*). These results indicate that the E-boxes of the *CYP3A7* and *CYP3A4* genes are recognized by USF1 in HepG2 cells.

We also performed a gel shift assay using BTE as a probe, because the sequence of this element is highly conserved among the P-450 genes and is believed to contribute to the basal promoter activity of the P-450 genes (53, 54). The sequence of the BTE region of the *CYP3A7* and *CYP3A4* genes perfectly fitted to degenerate Sp1 consensus sequence (Fig. 9*A*). As shown in Fig. 9*B*, three shifted bands (K, L, and M) appeared with the BTE region of the *CYP3A7* and *CYP3A4* genes. All three complexes disappeared after the addition of Sp1 consensus sequence. A mutated BTE, which had mutations within the core of an Sp1-binding sequence, did not affect the formation of the complexes. The addition of antibodies to Sp1 and Sp3 supershifted complex K and complexes L and M, respectively (Fig. 9*B*). These results indicate that the Sp family members interact with the BTE of the *CYP3A7* and *CYP3A4* genes in HepG2 cells.

Functional cis-Acting Elements for the CYP3A7 Proximal Promoter—To examine the roles of the HNF-3-binding site, NF1-binding site, USF1-binding site, and BTE on the promoter activity of the *CYP3A7* gene, mutations were introduced into these sites of a p3A7/−140 reporter construct by site-directed mutagenesis (Fig. 10*A*). The introduction of the mutation in the HNF-3-binding site, the USF1-binding site, or BTE reduced the promoter activity by 40, 40, or 50%, respectively, relative to the level seen with the p3A7/−140, whereas the mutation in the NF1-binding site increased the promoter activity. These results indicate that the HNF-3- and USF1-binding sites and BTE are required for the full activity of the proximal promoter. To further determine the relative contribution of each transcription factor in the transcriptional activation of the *CYP3A7* gene, *Drosophila* SL2 cells were co-transfected with expression plasmids, pPacSp1, pPacUSp3, pAcHNF-3β, or pAcUSF1 in combination with a reporter plasmid p3A7/−140 (Fig. 10*B*). Transfection with Sp1, Sp3, or USF1 activated the proximal promoter of the *CYP3A7* gene by ~10-fold. Although HNF-3β alone stimulated the promoter activity, the activity was enhanced by combination of HNF-3β with USF1, Sp1/Sp3, or both USF1 and Sp1/Sp3. Co-transfection with HNF-3β, Sp1, and USF1 enhanced the promoter activity by 43.6-fold. Thus, we conclude that transcription factors Sp1/Sp3, HNF-3β, and USF1 were critical factors for the maximal activity of the *CYP3A7* proximal promoter.

Synergism of Enhancer and Promoter—It was of interest to clarify a relationship between the NF-κB-like enhancer and the proximal promoter of the *CYP3A7* gene. Thus, we fused the distal enhancer region (−2500/−2250) encompassing the NF-κB-like element to promoters successively deleted as shown in Fig. 11*A*. Deletion from nucleotides −2000 to −360 increased the luciferase activity by 1.5-fold. Deletion of the HNF-3β-binding site, the USF1-binding site, and BTE in the proximal promoter region did not appreciably affect the enhancer-dependent activation of the *CYP3A7* gene, when the NF-κB-like enhancer was located close to TATA box (Fig. 11*A*). Thus, the minimal requirement for the NF-κB-like enhancer is likely to be a core promoter, TATA box, and/or initiator. Finally, we addressed the functional role of the proximal promoters in the

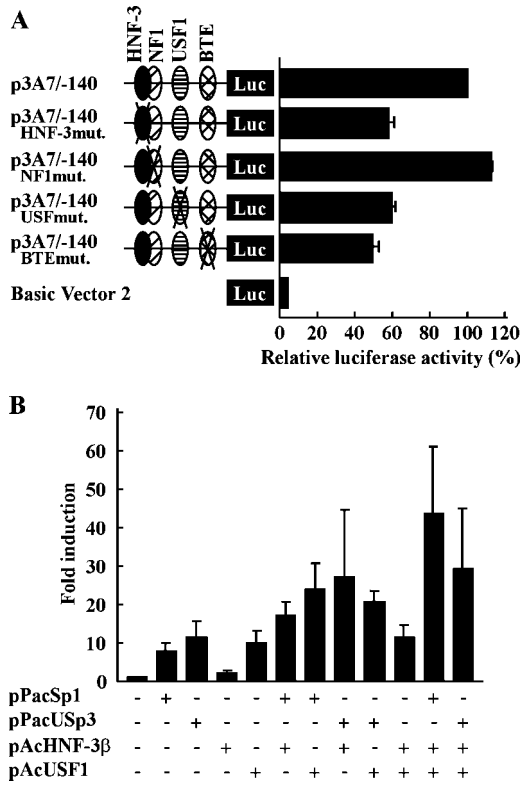

FIG. 10. **Functional roles of binding sites for HNF-3β, NF1, and USF1 and of BTE in the *CYP3A7* promoter activity.** *A*, effects of mutations in binding sites for HNF-3β, NF1, and USF1 and in BTE on the activity of the *CYP3A7* proximal promoter in HepG2 cells. The construction of mutant plasmids is described under "Experimental Procedures." HepG2 cells were transiently transfected with a reporter plasmid (8 μg). The values represent the averages ± S.D. from at least three independent experiments. The mean value obtained with p3A7/−140 is defined as 100%. *B*, expression plasmids, pPacSp1 (1 μg), pPacUSp3 (1 μg), pAcHNF-3β (1 μg), and/or pAcUSF1 (1 μg) were co-transfected to SL2 cells in combination with p3A7/−140 (4 μg). The results are expressed as fold induction relative to the activity obtained by co-transfection with the expression vector pPac as a control. The values represent the averages ± S.D. from at least three independent experiments.

context of the intact *CYP3A7* gene. Mutations were introduced into the HNF-3-binding site, the USF1-binding site, or BTE by site-directed mutagenesis (Fig. 11*B*). The mutation in the HNF-3-binding site, the USF1-binding site or BTE caused a 30−40% decrease in the NF-κB-like enhancer-dependent activity of the *CYP3A7* promoter. We also constructed the internal deletion mutant from nucleotides −360 to −35 of the p3A7/−2.5 (named p3A7/−2.5/Pdel.). The lack of the proximal promoter from nucleotides −360 to −35 decreased the promoter activity to 20% of the level seen with the p3A7/−2.5 only when the NF-κB-like enhancer was located distal to TATA box. Taking these results together, we conclude that synergism between the distal NF-κB-like enhancer and the proximal promoter is essential for the transcriptional activation of the *CYP3A7* gene in HepG2 cells.

DISCUSSION

A proposed model for the transcriptional regulation of the *CYP3A7* and *CYP3A4* genes in HepG2 cells is summarized in Fig. 12. We identified the binding sites of HNF-3β, NF1, YY1, USF1, and Sp1/Sp3 in the proximal promoters between nucleotides −140 and −35 of the *CYP3A7* and *CYP3A4* genes. HNF-4 has been reported as the constitutive activator of the rat *CYP3A2* and *CYP3A23* genes (55, 56). A binding site for HNF-4 was located in the upstream region between nucleotides −110 and −85 in the rat *CYP3A* genes. Although HNF-4-binding site was highly conserved in the mouse *Cyp3A11* (57) and *Cyp3a16* (58) genes, the element was not found in both the human *CYP3A7* and *CYP3A4* genes. Thus, HNF-4 may not be involved in the constitutive expression of the human *CYP3A* genes.

A binding site for a PXR/retinoid X receptor heterodimer has been identified as a xenobiotic-responsive enhancer in a region from nucleotides −168 to −148, which locates upstream the NF1-binding element, of the *CYP3A7* and *CYP3A4* genes (25–28). However, the functional roles of the PXR-responsive element in the constitutive expression of the two genes have not yet been clarified. Deletion of PXR-responsive elements from nucleotides −360 to −140 of the two genes increased luciferase activity by ~1.5-fold in HepG2 cells (Fig. 6*A*). Thus, PXR-responsive element may function as a negative regulatory element. Although a constitutive factor(s) that interacts with the PXR-responsive element remains to be identified, an orphan receptor COUP-TF (59), known to be a transcriptional repressor, is one of the candidates that constitutively bind to the PXR-responsive element. In fact, COUP-TF is reported to interact with the PXR-responsive element of the rat *CYP3A* genes, which contain the direct repeat of an AGGTCA motif separated by 3 nucleotides (called DR3) (56). Because COUP-TF is capable of recognizing the divergent types of the AGGTCA repeat (60, 61), COUP-TF may also interact with the ER6-type motif seen in the human *CYP3A* genes. Further detailed analysis is needed for understanding relationships between the PXR-responsive element and the elements identified in the present study.

We identified the novel NF-κB-like enhancer in the far upstream region between nucleotides −2330 and −2300 of the *CYP3A7* gene. The sequence of the NF-κB-like element (5′-GGGACTTGCC-3′) showed a 1-base pair mismatch as compared with the most typical NF-κB sequence (5′-GGGACTTTCC-3′) found in the Igκ gene. Recently, it was reported that a subset of NF-κB sequences, such as the NF-κB element of the Igκ gene, was recognized by a ubiquitous factor Sp1 (45). The dissociation constant of Sp1 for the NF-κB element of the Igκ gene was calculated to be 3.0×10^{-9} M. This value is comparable with the value calculated with the GC box of the Sp1-binding element. Although the dissociation constant of Sp1 for the *CYP3A7* NF-κB-like element remains to be determined, an enhancer activity seen with the concatenated *CYP3A7* NF-κB-like element was 10-fold higher than that seen with the concatenated NF-κB element of the Igκ gene in HepG2 cells (data not shown). In addition, the amount of the binding of Sp1 and Sp3 to the *CYP3A7* NF-κB-like element was decreased when guanine base at position 8 of the decameric sequence (5′-GGGACTTGCC-3′, defined 5′-end as position 1) was substituted to thymine base (Fig. 4*B*). Thus, the guanine base at position 8, which has not been seen in the NF-κB elements reported to date, may be important for a high affinity for Sp1. Although neither Sp1 nor Sp3 recognized the *CYP3A4* NF-κB-like element (5′-GGGACTTGAC-3′), the concatenated *CYP3A4* NF-κB-like element also showed an enhancer activity in HepG2 cells (Fig. 3*E*). This result indicates that an unknown factor(s), complex D, also acts as a transcriptional activator. Identification and characterization of complex D also remains to be elucidated.

Although Sp1 is regarded as a ubiquitous factor expressed in various cells, the expression level of Sp1 is regulated in cell type- and differentiation-specific manners. It has been reported that the expression level of Sp1 is elevated in fetal livers compared with the level seen in adult livers (62). Furthermore, the DNA binding activity of Sp1 is also down-regulated by the phosphorylation of Sp1 protein during the terminal differenti-

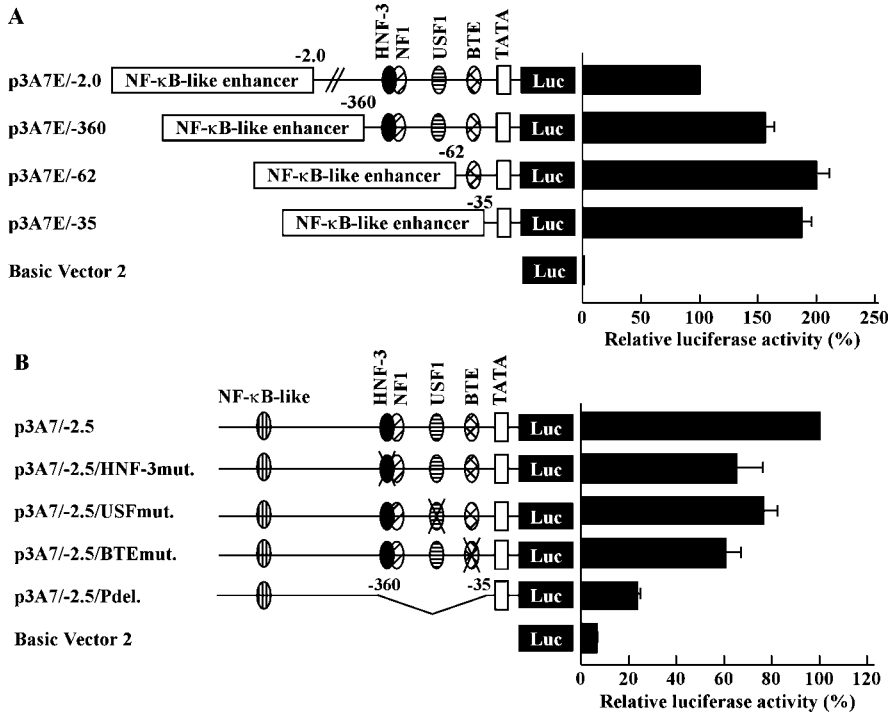

FIG. 11. **Synergism between the NF-κB-like enhancer and the proximal promoter of the *CYP3A7* gene in HepG2 cells.** *A*, roles of the proximal promoter in a short distance transactivation mediated by the NF-κB-like enhancer in the *CYP3A7* gene. The construction of internal deletion mutants is described under "Experimental Procedures." HepG2 cells (2×10^6 cells) were transiently transfected by the calcium phosphate coprecipitation method (37) with a reporter plasmid (8 μg). The values represent the averages ± S.D. from at least three independent experiments. The mean value obtained with p3A7E/−2.0 is defined as 100%. *B*, roles of the proximal promoter in a long distance transactivation mediated by the NF-κB-like enhancer in the intact *CYP3A7* promoter. The construction of mutant plasmids is described under "Experimental Procedures." The values represent the averages ± S.D. from at least three independent experiments. The mean value obtained with p3A7/−2.5 is defined as 100%.

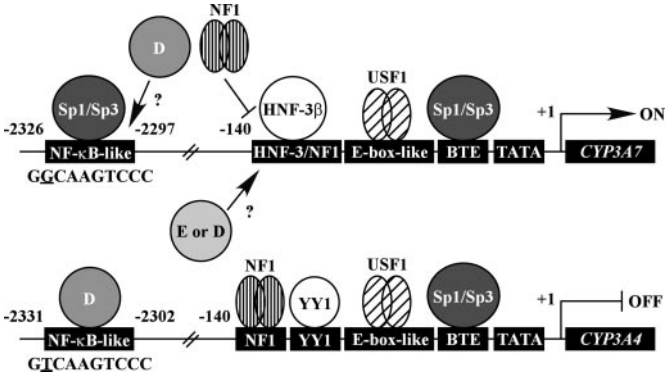

FIG. 12. **Possible model for the transcriptional regulation of the *CYP3A7* and *CYP3A4* genes.** The figure shows a schematic representation of binding sites for transcription factors functionally clarified in HepG2 cells. Only one 1-base pair mismatch (G/T) between the two genes exists in the NF-κB-like element. Transcriptional start sites (22, 23) are indicated by *+1*.

ation of hepatocytes (63). It is of particular interest to note that the *CYP3A7* NF-κB-like element is recognized by other unknown factors such as complex D besides Sp1. Complex D may also regulate the binding activity of Sp1 for the NF-κB-like element of the *CYP3A7* gene. Thus, the binding of Sp1 to the noncanonical NF-κB-like element may be involved in the fetus-specific activation of the *CYP3A7* promoter.

To date, three other Sp1-related proteins, Sp2 (64), Sp3 (46, 64), and Sp4 (46), have been identified. Sp3, like Sp1, is expressed in various cells. Sp3 can serve not only as a transcriptional activator but also as a repressor of Sp1-mediated transcription depending on cellular and promoter contexts (65, 66). In this study, we showed that Sp1 and Sp3 equally activated the *CYP3A7* promoter through the NF-κB-like element in SL2 cells. We employed an expression plasmid pPacUSp3, which was designed to express a full-length Sp3 protein (34). As shown in Fig. 4*D*, the *CYP3A7* NF-κB-like element was recognized by two Sp3 isoforms to generate complexes B and C. Complex C is likely to be formed by binding with Sp3 (p80), which is translated from two internal AUGs located within Q-rich activation domain B (67). The Sp3 (p80) isoform lacks Q-rich activation domain A and thereby has little or no capacity to stimulate transcription. Thus, Sp3 (p80) may inhibit the transcriptional activation of the *CYP3A7* promoter by Sp1 and intact Sp3 isoform.

The gel shift assay and the introduction of mutations by site-directed mutagenesis demonstrated that HNF-3β and USF1, in addition to the members of the Sp family, functioned as the activators of the *CYP3A7* proximal promoter. The activity of the liver-specific promoter such as α-fetoprotein and albumin promoters has been reported to be controlled by the combined action of the liver-enriched transcription factors, including C/EBP, D site-binding protein, HNF-1, HNF-3, HNF-4, and HNF-6 (68). Among them, HNF-3 isoforms, HNF-3α, HNF-3β, and HNF-3γ, which are known to be a subgroup of winged helix factors, are expressed at the early stage of embryonic development (69–71). Thus, HNF-3 isoforms are thought to be primary factors in the hierarchy of the expression of liver-enriched transcription factors during liver development (72, 73). It should be noted that the *CYP3A7* gene is also expressed at the early stages of embryonic livers at 50–60 days of gestation. In addition, the HNF-3 family contains a winged helix DNA-binding motif similar to the three-dimensional structure of the globular domain of linker histone (74). Thus, HNF-3 stably binds to the linker histone site on nucleosome. For instance, the binding of HNF-3 to the enhancer identified in the albumin gene causes the change of nucleosome positioning and then triggers the assembly of an enhancer complex on silent chromatin (75–77). USF1, which is one of the activators of the *CYP3A7* promoter, cannot interact with histone H1-binding nucleosome (78). Thus, HNF-3 but not USF1 may play a key role in the activation of the *CYP3A7* promoter at a chromatin level at the early stage of liver development in human fetuses.

The binding site of HNF-3 perfectly overlapped with that of NF1 in the *CYP3A7* gene. Similarly, overlapped or nearby binding sites for HNF-3 and NF1 proteins have been found in some liver-specific promoters such as the albumin and the *C4BPβ* (C4b-binding protein β-chain) genes (79, 80). In such a promoter, NF1 cooperatively interacts with HNF-3 to activate the transcription of the gene in the liver. However, we demonstrated that this was not the case for the *CYP3A7* gene, because

introduction of mutations into the NF1-binding site slightly increased promoter activity. This result indicates that NF1 can repress the activity of the *CYP3A7* promoter by competing the binding sites with HNF-3. Unlike the *CYP3A7* gene, the NF1-binding site of the *CYP3A4* gene was located close to the binding site of YY1, which is known to be a transcriptional repressor (81, 82). Although the functional role(s) of the NF1-binding site on the *CYP3A4* promoter remains to be clarified, NF1 may function as the transcriptional activator of the *CYP3A4* gene by interfering with YY1. Thus, NF1 may be responsible for the age-related expression of the *CYP3A7* and *CYP3A4* genes, because the expression of NF1 is reported to be up-regulated postnatally (83, 84).

E-box, CANNTG, is reported to be a target element for the basic helix-loop-helix family such as USF1, USF2, MyoD, Myc, Max, TFE3, and E47 (48). In this study, we showed that USF1 was the major protein bound to the noncanonical E-box sites of the *CYP3A7* and *CYP3A4* genes in HepG2 cells. Complex J, which appeared with the E-box sites of the *CYP3A7* and *CYP3A4* genes as probes, was supershifted by the addition of antibodies to USF1. In HepG2 cells, the USF1/USF2 heterodimer is reported to be predominant, *i.e.* ~76% of the total USF binding activity (85). Thus, USF2 may be involved in the activation of the *CYP3A7* and *CYP3A4* promoters. Although USF1 bound to the E-box sites of both the *CYP3A7* and *CYP3A4* genes, the level of luciferase activity differed between the two p3A7/−90 and p3A4/−90 reporter plasmids (Fig. 6*A*). Other basic helix-loop-helix proteins besides USF1 and USF2 may be used to recognize the E-box in the *CYP3A4* gene. The binding activity of USF1 for E-box is reported to be increased by C/EBPα (86). It has also been reported that the level of C/EBPα is high in mature hepatocytes but is low in hepatoma cells such as HepG2 cells (87). Combining these lines of evidence, the low activity of the *CYP3A4* promoter in HepG2 cells may be explained, at least in part, by the low binding activity of USF1.

The NF-κB-like element of the *CYP3A7* gene is unique in that a long distance transactivation by Sp1 occurred through the element, although previous studies have demonstrated that Sp1 functions as a "proximal" activator (88). Sp1 can stimulate transcription only from a position close to TATA box. Although the mechanism(s) by which Sp1 transactivates the *CYP3A7* promoter from approximately −2.3 kb upstream of the transcription start site remains to be defined, our preliminary experiments indicate that other unknown factors interacting with the NF-κB-like element are also necessary for the long distance activation. Thus, the conformation of Sp1 and/or a co-factor(s) interacting with Sp1 may differ between the NF-κB-type motif and the GC box-type motif.

Acknowledgments—We thank Dr. Robert Tjian, Dr. Guntram Susuke, and Dr. Naoko Tanese for generously providing Sp1 and Sp3 expression plasmids and anti-NF1 antibodies, respectively, and Dr. Robert H. Costa for HNF-3 expression plasmids and anti-HNF-3 antibodies. We are grateful to Dr. Hiroyoshi Ariga, Dr. Takahiro Taira, and Dr. Hidekazu Nakabayashi of Hokkaido University and Dr. Shinichi Kudo of Hokkaido Institute of Public Health for valuable discussions.

REFERENCES

1. Wrighton, S. A., and Stevens, J. C. (1992) *Crit. Rev. Toxicol.* **22,** 1–21
2. Nelson, D. R., Koymans, L., Kamataki, T., Stegeman, J. J., Feyereisen, R., Waxman, D. J., Waterman, M. R., Gotoh, O., Coon, M. J., Estabrook, R. W., Gunsalus, I. C., and Nebert, D. W. (1996) *Pharmacogenetics* **6,** 1–42
3. Kitada, M., Kamataki, T., Itahashi, K., Rikihisa, T., Kato, R., and Kanakubo, Y. (1985) *Biochem. Biophys. Res. Commun.* **131,** 1154–1159
4. Kitada, M., and Kamataki, T. (1979) *Biochem. Pharmacol.* **28,** 793–797
5. Beaune, P. H., Umbenhauer, D. R., Bork, R. W., Lloyd, R. S., and Guengerich, F. P. (1986) *Proc. Natl. Acad. Sci. U. S. A.* **83,** 8064–8068
6. Gonzalez, F. J., Schmid, B. J., Umeno, M., Mcbride, O. W., Hardwick, J. P., Meyer, U. A., Gelboin, H. V., and Idle, J. R. (1988) *DNA* **7,** 79–86
7. Bork, R. W., Muto, T., Beaune, P. H., Srivastava, P. K., Lloyd, R. S., and Guengerich, F. P. (1989) *J. Biol. Chem.* **264,** 910–919
8. Aoyama, T., Yamano, S., Waxman, D. J., Lapenson, D. P., Meyer, U. A., Fischer, V., Tyndale, R., Inaba, T., Kalow, W., and Gelboin, H. V. (1989) *J. Biol. Chem.* **264,** 10388–10395
9. Schuetz, J. D., Molowa, D. T., and Guzelian, P. S. (1989) *Arch. Biochem. Biophys.* **274,** 355–365
10. Komori, M., Nishio, K., Ohi, H., Kitada, M., and Kamataki, T. (1989) *J. Biochem.* **105,** 161–163
11. Domanski, T. L., Finta, C., Halpert, J. R., and Zaphiropoulos, P. G. (2001) *Mol. Pharmacol.* **59,** 386–392
12. Kitada, M., Kamataki, T., Itahashi, K., Rikihisa, T., and Kanakubo, Y. (1987) *Biochem. Pharmacol.* **36,** 453–456
13. Kitada, M., Kamataki, T., Itahashi, K., Rikihisa, T., and Kanakubo, Y. (1987) *J. Biol. Chem.* **262,** 13534–13537
14. Kitada, M., Kamataki, T., Itahashi, K., Rikihisa, T., Kato, R., and Kanakubo, Y. (1985) *Arch. Biochem. Biophys.* **241,** 275–280
15. Hashimoto, H., Nakagawa, T., Yokoi, T., Sawada, M., Itoh, S., and Kamataki, T. (1995) *Cancer Res.* **55,** 787–791
16. Li, Y., Yokoi, T., Kitamura, R., Sasaki, M., Gunji, M., Katsuki, M., and Kamataki, T. (1996) *Arch. Biochem. Biophys.* **329,** 235–240
17. Li, Y., Yokoi, T., Katsuki, M., Wang, J. S., Groopman, J. D., and Kamataki, T. (1997) *Cancer Res.* **57,** 641–645
18. Komori, M., Nishio, K., Kitada, M., Shiramatsu, K., Muroya, K., Soma, M., Nagashima, K., and Kamataki, T. (1990) *Biochemistry* **29,** 4430–4433
19. Schuetz, J. D., Beach, D. L., and Guzelian, P. S. (1994) *Pharmacogenetics* **4,** 11–20
20. Yang, H. Y., Lee, Q. P., Rettie, A. E., and Juchau, M. R. (1994) *Mol. Pharmacol.* **46,** 922–928
21. Lacroix, D., Sonnier, M., Moncion, A., Cheron, G., and Cresteil, T. (1997) *Eur. J. Biochem.* **247,** 625–634
22. Itoh, S., Yanagimoto, T., Tagawa, S., Hashimoto, H., Kitamura, R., Nakajima, Y., Okouchi, T., Fujimoto, S., Uchino, J., and Kamataki, T. (1992) *Biochim. Biophys. Acta* **1130,** 133–138
23. Hashimoto, H., Toide, T., Kitamura, R., Fujita, M., Tagawa, S., Itoh, S., and Kamataki, T. (1993) *Eur. J. Biochem.* **218,** 585–595
24. Maurel, P. (1996) in *Cytochromes P-450: Metabolic and Toxicological Aspects* (Ioannides, C., ed) pp. 241–270, CRC Press, Boca Raton, FL
25. Lehmann, J. M., McKee, D. D., Watson, M. A., Willson, T. M., Moor, J. T., and Kliewer, S. A. (1998) *J. Clin. Invest.* **102,** 1016–1023
26. Blumberg, B., Sabbagh, W., Jr., Juguilon, H., Bolado, J., Jr., van Meter, C. M., Ong, E. S., and Evans, R. M. (1998) *Genes Dev.* **12,** 3195–3205
27. Bertilsson, G., Heidrich, J., Svensson, K., Åsman, M., Jendeberg, L., Sydow-Bäckman, M., Ohlsson, R., Postlind, H., Blomquist, P., and Berkenstam, A. (1998) *Prot. Natl. Acad. Sci. U. S. A.* **95,** 12208–12213
28. Pascussi, J. M., Jounaidi, Y., Drocourt, L., Domergue, J., Balabaud, C., Maurel, P., and Vilarem, M. J. (1999) *Biochem. Biophys. Res. Commun.* **260,** 377–381
29. Xie, W., Barwick, J. L., Downes, M., Blumberg, B., Simon, C. M., Nelson, M. C., Neuschwander-Tetri, B. A., Brunt, E. M., Guzelian, P. S., and Evans, R. M. (2000) *Nature* **406,** 435–439
30. Kelly, J. H., and Darlington, G. J. (1989) *In Vitro Cell. Dev. Biol.* **25,** 217–222
31. Chomczynski, P., and Sacchi, N. (1987) *Anal. Biochem.* **162,** 156–159
32. Hakkola, J. M., Pasanen, M., Hukkanen, J., Pelkonen, O., Mäenpää, J., Edwards, R. J., Boobis, A. R., and Raunio, H. (1996) *Biochem. Pharmacol.* **51,** 403–411
33. Courey, A. J., and Tjian, R. (1988) *Cell* **55,** 887–898
34. Dennig, J., Beato, M., and Suske, G. (1996) *EMBO J.* **15,** 5659–5667
35. Lai, E., Prezioso, V. R., Tao, W. F., Chen, W. S., and Darnell, J. E., Jr. (1991) *Genes Dev.* **5,** 416–427
36. Takahashi, Y., Nakayama, K., Itoh, S., Fujii-Kuriyama, Y., and Kamataki, T. (1997) *J. Biol. Chem.* **272,** 30025–30031
37. Sambrook, J., Fritsch, E. F., and Maniatis, T. (1989) *Molecular Cloning*: *A Laboratory Manual*, 2nd Ed., Cold Spring Harbor Laboratory, Cold Spring Harbor, NY
38. Kudo, S. (1998) *Mol. Cell. Biol.* **18,** 5492–5499
39. Dignam, J. D., Levovitz, R. M., and Roeder, R. G. (1983) *Nucleic Acids Res.* **11,** 1475–1489
40. Sen, R., and Baltimore, D. (1986) *Cell* **46,** 705–716
41. Clark, L., Pollock, R. M., and Hay, R. (1988) *Genes Dev.* **8,** 991–1002
42. Shibuya, H., Yoneyama, M., and Taniguchi, T. (1989) *Int. Immunol.* **1,** 43–49
43. Baldwin, A. S., and Sharp, P. A. (1988) *Proc. Natl. Acad. Sci. U. S. A.* **85,** 723–727
44. Brasier, A. R., Ron, D., Tate, J. E., and Habener, J. F. (1990) *EMBO J.* **9,** 3933–3944
45. Hirano, F., Tanaka, H., Hirano, Y., Hiramoto, M., Handa, H., Makino, I., and Scheidereit, C. (1998) *Mol. Cell. Biol.* **18,** 1266–1274
46. Hagen, G., Müller, S., Beato, M., and Suske, G. (1992) *Nucleic Acids Res.* **20,** 5519–5525
47. Hansen, S. K., Baeuerle, P. A., and Blasi, F. (1994) *Mol. Cell. Biol.* **14,** 2593–2603
48. Massari, M. E., and Murre, C. (2000) *Mol. Cell. Biol.* **20,** 429–440
49. Shih, H.-M., Liu, Z., and Towle, H. C. (1995) *J. Biol. Chem.* **270,** 21991–21997
50. Chodosh, L. A., Carthew, R. W., Morgan, J. G., Crabtree, G. R., and Sharp, P. A. (1987) *Science* **238,** 684–688
51. Bresnick, E. H., and Felsenfeld, G. (1993) *J. Biol. Chem.* **268,** 18824–18834
52. Sawadogo, M., and Roeder, R. G. (1985) *Cell* **43,** 165–175
53. Yanagida, A., Sogawa, K., Yasumoto, K., and Fujii-Kuriyama, Y. (1990) *Mol. Cell. Biol.* **10,** 1470–1475
54. Imataka, H., Sogawa, K., Yasumoto, K., Kikuchi, Y., Sasano, K., Kobayashi, A., Hayami, M., and Fujii-Kuriyama, Y. (1992) *EMBO J.* **10,** 3663–3671
55. Miyata, M., Nagata, K., Yamazoe, Y., and Kato, R. (1995) *Arch. Biochem. Biophys.* **318,** 71–79
56. Huss, J. M., and Kasper, C. B. (1998) *J. Biol. Chem.* **273,** 16155–16162
57. Toide, K., Itoh, S., Nagasaka, Y., Yanagimoto, T., and Kamataki, T. (1997)

Arch. Biochem. Biophys. **338,** 43–49
58. Itoh, S., Abe, Y., Kubo, A., Okuda, M., Shimoji, M., Nakayama, K., and Kamataki, T. (1997) *Biochim. Biophys. Acta* **1350,** 155–158
59. Tsai, S. Y., and Tsai, M.-J. (1997) *Endocr. Rev.* **18,** 229–240
60. Cooney, A. J., Tsai, S. Y., O'Malley, B. W., and Tsai, M.-J. (1992) *Mol. Cell. Biol.* **12,** 4153–4163
61. Kadowaki, Y., Toyoshima, K., and Yamamoto, T. (1992) *Biochem. Biophys. Res. Commun.* **183,** 492–498
62. Saffer, J. D., Jackson, S. P., and Annarella, M. B. (1991) *Mol. Cell. Biol.* **11,** 2189–2199
63. Leggett, R. W., Armstrong, S. A., Barry, D., and Mueller, C. R. (1995) *J. Biol. Chem.* **270,** 25879–25884
64. Kingsley, C., and Winoto, A. (1992) *Mol. Cell. Biol.* **12,** 4251–4261
65. Hagen, G., Müller, S., Beato, M., and Suske, G. (1994) *EMBO J.* **13,** 3843–3851
66. Suske, G. (1999) *Gene* (*Amst.*) **238,** 291–300
67. Kennett, S. B., Udvadia, A. J., and Horowitz, J. M. (1997) *Nucleic Acids Res.* **25,** 3110–3117
68. Tronche, F., and Yaniv, M. (1994) *Liver Gene Expression*, Landes, Austin, TX
69. Ang, S. L., Wierda, L. A., Wong, K. A., Stevens, K. A., Cascio, S., Rossant, J., and Zaret, K. S. (1993) *Development* **119,** 1301–1315
70. Monaghan, A. P., Kaestner, K. H., Grau, E., and Schütz, G. (1993) *Development* **119,** 567–578
71. Sasaki, H., and Hogan, B. L. (1993) *Development* **118,** 47–59
72. Duncan, S. A., Navas, M. A., Dufort, D., Rossant, J., and Stoffel, M. (1998) *Science* **281,** 692–695
73. Hayashi, Y., Wang, W., Ninomiya, T., Nagano, H., Ohta, K., and Itoh, H. (1999) *Mol. Pathol.* **52,** 19–24
74. Clark, K. L., Halay, E. D., Lai, E., and Burley, S. K. (1993) *Nature* **364,** 412–420
75. McPherson, C. E., Shim, E.-Y., Friedman, D. S., and Zaret, K. S. (1993) *Cell* **75,** 387–398
76. Cirillo, L. A., McPherson, C. E., Bossard, P., Stevens, K., Cherian, S., Shim, E.-Y., Clark, K. L., Burley, S. K., and Zaret, K. S. (1998) *EMBO J.* **17,** 244–254
77. Cirillo, L. A., and Zaret, K. S. (1999) *Mol. Cell* **4,** 961–969
78. Juan, L.-J., Utley, R. T., Adams, C. C., Vetteese-Dadey, M., and Workman, J. L. (1994) *EMBO J.* **13,** 6031–6040
79. Jackson, D. A., Rowader, K. E., Stevens, K., Jiang, C., Milos, P., and Zaret, K. S. (1993) *Mol. Cell. Biol.* **13,** 2401–2410
80. Arenzana, N., and Rodrigues de Cordoba, S. (1996) *J. Immunol.* **156,** 168–175
81. Shi, Y., Lee, J.-S., and Galvin, K. M. (1997) *Biochim. Biophys. Acta* **1332,** F49–F66
82. Thomas, M. J., and Seto, E. (1999) *Gene* (*Amst.*) **236,** 197–208
83. Puzianowska-Kuznicka, M., and Shi, Y.-B. (1996) *J. Biol. Chem.* **271,** 6273–6282
84. Chaudhry, A. Z., Lyons, G. E., and Gronostajski, R. M. (1997) *Dev. Dyn.* **208,** 313–325
85. Viollet, B., Lefrançis-Martinez, A.-M., Henrion, A., Kahn, A., Raymondjean, M., and Martinez, A. (1996) *J. Biol. Chem.* **271,** 1405–1415
86. Timchenko, N., Wilson, D. R., Taylor, L. R., Abdelsayed, S., Wilde, M., Sawadogo, M., and Darlington, G. J. (1995) *Mol. Cell. Biol.* **15,** 1192–1202
87. Friedman, A. D., Landschulz, W. H., and McKnight, S. L. (1989) *Genes Dev.* **3,** 1314–1322
88. Seipel, K., Georgiev, O., and Schaffner, W. (1992) *EMBO J.* **11,** 4961–4968
89. Grilli, M., Chiu, J. J., and Lenardo, M. J. (1993) *Int. Rev. Cytol.* **143,** 1–62
90. Zabel, U., Schreck, R., and Baeuerle, P. A. (1991) *J. Biol. Chem.* **266,** 252–260